Phosphinoferrocenyl Carboxamides Bearing Glycine Pendant Groups: Synthesis, Palladium(II) Complexes, and Catalytic Use in Polar and Aqueous Reaction Media

Jiří Tauchman, Ivana Císařová, and Petr Štěpnička*

Department of Inorganic Chemistry, Faculty of Science, Charles University in Prague, Hlavova 2030, 128 40 Prague, Czech Republic

Received March 19, 2009

The reaction of 1′-(diphenylphosphino)-1-ferrocenecarboxylic acid (Hdpf) with $H_2NCH_2CO_2CR_3$ mediated by peptide coupling agents (EDC/HOBt) afforded novel glycine phosphino-carboxamides $Ph_2PfcCONHCH_2CO_2CR_3$ (fc = ferrocene-1,1′-diyl; R = H (**1**) and Me (**2***)). Compound **1** was converted to its corresponding phosphine oxide (**3***) and sulfide (**4***), to *N*-acyl glycine $Ph_2PfcCONHCH_2CO_2H$ (**5**), and to bis-amide $Ph_2PfcCONHCH_2CONH_2$ (**6***). Compounds **1** and **6** reacted with $[PdCl_2(cod)]$ (cod = η^2:η^2-cycloocta-1,5-diene) and **5** reacted with $Na_2[PdCl_4]$ to afford the respective, mostly solvated bis-phosphine complexes *trans*-$[PdCl_2(L\text{-}\kappa P)_2]$ (**7**: L = **1**; **8**: L = **5**, **9**: L = **6**). Two different solvatomorphs of **9** were isolated in crystalline form and structurally characterized (**9*** and **9a***). Furthermore, bridge cleavage reaction of $[\{Pd(\mu\text{-}Cl)(L^{NC})\}_2]$ (L^{NC} = 2-[(dimethylamino-κN)methyl]phenyl-κC^1) with **1** gave $[(L^{NC})Pd(Cl)(\mathbf{1}\text{-}\kappa P)]$ (**10***), which was further reacted with $AgClO_4$ or KO*t*-Bu to afford bis-chelate complexes $[(L^{NC})Pd(\mathbf{1}\text{-}\kappa^2 O,P)]ClO_4$ (**11***) and $[(L^{NC})Pd(L\text{-}\kappa^2 N,P)]$ (**12***; L = **1** deprotonated at the NH group), respectively. All compounds were characterized by spectroscopic methods (multinuclear NMR, MS, and IR) and by elemental analyses; the asterisk indicates that the crystal structure has been determined. Compounds **1**, **3**−**6**, and **10**−**12** were studied by electrochemical methods, while phosphines **1**, **5**, and **6** in combination with palladium(II) acetate were shown to be highly active catalysts for the Suzuki−Miyaura cross-coupling of aryl bromides with phenylboronic acid in polar solvents (ethanol and dioxane), in their aqueous mixtures, and in pure water.

Introduction

Conjugation of ferrocenecarboxylic acids with amino acids or peptides via amide bonds represents a convenient method for introduction of the ferrocene moiety into biomolecules. A vast number of such conjugates have been prepared from ferrocenecarboxylic and 1,1′-ferrocenedicarboxylic acids mainly for redox labeling or structural studies,[1] while only little has been done with ferrocenecarboxylic acids possessing additional functional groups.[2] While studying the chemistry of 1′-(diphenylphosphino)-1-ferrocenecarboxylic acid (Hdpf)[3] and the related acids,[4,5] we found that they can be readily converted to simple and N-functionalized phosphine-carboxamides.[6,7] The possibility of changing the substituents at the amide nitrogen part makes these compounds highly versatile. So far, they were demonstrated to be valuable synthetic building blocks[8] and flexible ligands for coordination chemistry and catalysis.[6,7] The latter application fields can particularly benefit from fine-tuning of the ligand properties by means of substituents in the amide

* Corresponding author. E-mail: stepnic@natur.cuni.cz.

(1) Selected reviews: (a) Metzler-Nolte, N.; Salmain, M. *The Bioorganometallic Chemistry of Ferrocene in Ferrocenes: Ligands, Materials and Biomolecules*; Štěpnička, P., Ed.; Wiley: Chichester, 2008; Chapter *13*, pp 499−639. (b) Heinze, K.; Beckmann, M.; Hempel, K. *Chem.*−*Eur. J.* **2008**, *14*, 9468. (c) Moriuchi, T.; Hirao, T. *Top. Organomet. Chem.* **2006**, *17*, 143. (d) Kraatz, H.-B. *J. Inorg. Organomet. Polym. Mater.* **2005**, *15*, 83. (e) van Staveren, D. R.; Metzler-Nolte, N. *Chem. Rev.* **2004**, *104*, 5931. (f) Moriuchi, T.; Hirao, T. *Chem. Soc. Rev.* **2004**, *33*, 294.

(2) Several bis(peptidyl) derivatives of 1′-amino-1-ferrocenecarboxylic acid were reported (refs 1a and 1b).

(3) Podlaha, J.; Štěpnička, P.; Císařová, I.; Ludvík, J. *Organometallics* **1996**, *15*, 543.

(4) (a) Štěpnička, P. *Eur. J. Inorg. Chem.* **2005**, 3787. (b) Štěpnička, P. *1′-Functionalised Ferrocene Phosphines: Synthesis, Coordination Chemistry and Catalytic Applications in Ferrocenes: Ligands, Materials and Biomolecules*; Štěpnička, P., Ed.; Wiley, Chichester, 2008; Chapter 5, pp 177−204.

(5) Recent examples: (a) Lamač, M.; Císařová, I.; Štěpnička, P. *New J. Chem.* **2009**, *33*, doi: 10.1039/b901262a. (b) Lamač, M.; Cvačka, J.; Štěpnička, P. *J. Organomet. Chem.* **2008**, *693*, 3430. (c) Bianchini, C.; Meli, A.; Oberhauser, W.; Segarra, A. M.; Passaglia, E.; Lamač, M.; Štěpnička, P. *Eur. J. Inorg. Chem.* **2008**, 441. (d) Kühnert, J.; Lamač, M.; Rüffer, T.; Walfort, B.; Štěpnička, P.; Lang, H. *J. Organomet. Chem.* **2007**, *692*, 4303. (e) Lamač, M.; Císařová, I.; Štěpnička, P. *Collect. Czech. Chem. Commun.* **2007**, *72*, 985. (f) Lamač, M.; Císařová, I.; Štěpnička, P. *Eur. J. Inorg. Chem.* **2007**, 2274. (g) Štěpnička, P.; Císařová, I. *Collect. Czech. Chem. Commun.* **2006**, *71*, 279. (h) Lamač, M.; Císařová, I.; Štěpnička, P. *J. Organomet. Chem.* **2005**, *690*, 4285. (i) Trzeciak, A. M.; Štěpnička, P.; Mieczyńska, E.; Ziółkowski, J. *J. Organomet. Chem.* **2005**, *690*, 3260.

(6) (a) Schulz, J.; Císařová, I.; Štěpnička, P. *J. Organomet. Chem.* **2009**, *694*, doi: 10.1016/j.jorganchem.2009.04.007. (b) Kühnert, J.; Císařová, I.; Lamač, M.; Štěpnička, P. *Dalton Trans.* **2008**, 2454. (c) Kühnert, J.; Lamač, M.; Demel, J.; Nicolai, A.; Lang, H.; Štěpnička, P. *J. Mol. Catal. A: Chem.* **2008**, *285*, 41. (d) Lamač, M.; Tauchman, J.; Císařová, I.; Štěpnička, P. *Organometallics* **2007**, *26*, 5042. (e) Kühnert, J.; Dušek, M.; Demel, J.; Lang, H.; Štěpnička, P. *Dalton Trans.* **2007**, 2802. (f) Štěpnička, P.; Schulz, J.; Císařová, I.; Fejfarová, K. *Collect. Czech. Chem. Commun.* **2007**, *72*, 453. See also refs 5a and 5f.

(7) For further examples, see: (a) Zhang, W.; Shimanuki, T.; Kida, T.; Nakatsuji, Y.; Ikeda, I. *J. Org. Chem.* **1999**, *64*, 6247. (b) Longmire, J. M.; Wang, B.; Zhang, X. *J. Am. Chem. Soc.* **2002**, *124*, 13400. (c) You, S.-L.; Hou, X.-L.; Dai, L.-X. *J. Organomet. Chem.* **2001**, *637*−*639*, 762. (d) You, S.-L.; Hou, X.-L.; Dai, L.-X.; Zhu, X.-Z. *Org. Lett.* **2001**, *3*, 149. (e) Longmire, J. M.; Wang, B.; Zhang, X. *Tetrahedron Lett.* **2000**, *41*, 5435. (f) You, S.-L.; Hou, X.-L.; Dai, L.-X.; Cao, B.-X.; Sun, J. *Chem. Commun.* **2000**, 1933.

(8) (a) Meca, L.; Dvořák, D.; Ludvík, J.; Císařová, I.; Štěpnička, P. *Organometallics* **2004**, *23*, 2541. (b) Drahoňovský, D.; Císařová, I.; Štěpnička, P.; Dvořáková, H.; Maloň, P.; Dvořák, D. *Collect. Czech. Chem. Commun.* **2001**, *66*, 588.

10.1021/om900209j CCC: $40.75
Publication on Web 05/13/2009

part. For instance, introduction of additional donor moieties was shown to increase the range of accessible coordination modes and may impart hemilabile coordination,[9] while polar groups render the amidophosphines (and their complexes) more soluble in polar solvents.[6a,10]

This led us to design *ferrocene* phosphinocarboxamides derived from amino acids that, to the best of our knowledge, were not reported to date. Indeed, organic phosphine-substituted amino acids are in no way unprecedented. Yet, they were typically prepared by direct synthesis and manipulation of amino acid side chains[11,12] or, alternatively, by Mannich condensation from amino acids, formaldehyde, and secondary phosphines (or hydroxymethylphosphines) to give *N*-(phosphinomethyl) amino acids.[13] By contrast, the straightforward approach making use of amidation reactions with phosphinocarboxylic acids remains still less explored[14] despite holding considerable synthetic potential, mainly for the preparation of multidentate ligands with great structural and coordination variability that can be advantageously applied in coordination chemistry and catalysis.

With this contribution, we report the preparation and structural characterization of the first phosphinoferrocene-carboxamides with glycine-based pendant groups (Gly-OH, Gly-OR, Gly-NH_2) obtained by "conjugation" of Hdpf with glycine esters (Gly-OR) and subsequent transformations at the phosphinoferrocenyl group and in the glycine moiety. Also reported are the preparation and crystal structures of several palladium(II) complexes with these hybrid donors, electrochemical characterization of the compounds, and the results of their catalytic testing in Suzuki−Miyaura cross-coupling reaction.

Results and Discussion

Synthesis of Glycine-amides. Conjugates of ferrocenecarboxylic acids with amino acids or peptides are typically prepared by the direct reaction mediated by peptide coupling agents.[1] Because of high yields and mild reaction conditions, this method was employed also for the preparation of Hdpf-glycine amides.[15] Thus, compounds **1** and **2** were synthesized by the coupling of respective glycine esters, H-Gly-OMe and H-Gly-O*t*-Bu (generated *in situ* from their hydrochlorides and triethylamine), to Hdpf in the presence of 1-hydroxybenzotriazole and *N*-[3-(dimethylamino)propyl]-*N*′-ethylcarbodiimide (Scheme 1). The amides were purified by column chromatography and isolated as air-stable orange solids in excellent yields and were characterized by conventional spectral methods and by combustion analysis. The crystal structure of **2** was determined by single-crystal X-ray diffraction.

$^{31}P\{^1H\}$ NMR resonances of **1** and **2** are found at positions similar to free Hdpf,[3] while the glycine CH_2 groups are observed as NH-coupled doublets at δ_H ca. 4.0 in ^1H NMR and singlets at δ_C 41−42 in $^{13}C\{^1H\}$ NMR spectra. The NMR spectra further comprise characteristic signals due to the phosphinoferrocene moiety and a pair of C═O resonances at δ_C ca. 170. The presence of the ester and amide groups is further manifested by their diagnostic bands in IR spectra. Compounds **1** and **2** are thermally robust, showing abundant molecular ions in electron-impact mass spectra. Their fragmentation pathways are similar, involving the elimination of OCR_3 and $CH_2CO_2CR_3$ radicals (R = H and Me) and disintegration of the phosphinoferrocene unit.[16]

Compound **1** was subsequently modified at the phosphine moiety and in the pendant glycine substituent (Scheme 1). Oxidation with hydrogen peroxide or with sulfur produced the corresponding phosphine oxide (**3**) and sulfide (**4**) in practically quantitative yields after crystallization or chromatography, respectively. Hydrolysis of **1** with NaOH in dioxane/water followed by acidification also proceeded cleanly to afford *N*-acyl glycine **5**. Isolation by column chromatography provided the acid in a very good yield and reasonable purity. Exhaustive purification of **5** proved difficult, as the acid is notoriously contaminated with traces of its corresponding phosphine oxide, which coelutes during the chromatography and cannot be removed by crystallization (*N.B.* Acid **5** is reluctant to crystallize). Finally, treatment of a methanolic solution of **1** with liquid ammonia gave bis-amide **6**, which was isolated in 88% yield after chromatography and crystallization. Compounds **3**−**6** were

(9) (a) Braunstein, P.; Naud, F. *Angew. Chem., Int. Ed.* **2001**, *40*, 680. (b) Slone, C. S.; Weinberger, D. A.; Mirkin, C. A. *Prog. Inorg. Chem.* **1999**, *48*, 233. (c) Bader, A.; Lindner, E. *Coord. Chem. Rev.* **1991**, *108*, 27.

(10) (a) *Aqueous-Phase Organometallic Catalysis*, 2nd ed.; Cornils, B., Herrmann, W. A., Eds.; Wiley-VCH: Weinheim, 2004. (b) Joó, F. *Aqueous Organometallic Catalysis*; Kluwer: New York, 2002.

(11) Selected examples: (a) Meyer, C.; Scherer, M.; Schönberg, H.; Rüegger, H.; Loss, S.; Gramlich, V.; Grützmacher, H. *Dalton Trans.* **2006**, 137. (b) Heinicke, J.; Peulecke, N.; Jones, P. G. *Chem. Commun.* **2005**, 262. (c) Agarkov, A.; Greenfield, S.; Xe, D.; Pawlick, R.; Starkey, G.; Gilbertson, S. R. *Biopolymers* **2005**, *84*, 48. (d) Iyengar, V.; Galka, P. V.; Pletsch, A.; Kraatz, H.-B. *Can. J. Chem.* **2002**, *80*, 1562. (e) Greenfield, S. J.; Gilbertson, S. R. *Synthesis* **2001**, 2337. (f) Brauer, D. J.; Kottsieper, K. W.; Schenk, S.; Stelzer, O. *Z. Anorg. Allg. Chem.* **2001**, *627*, 1151. (g) Kratz, H.-B.; Pletsch, A. *Tetrahedron: Asymmetry* **2000**, *11*, 1617. (h) Gilbertson, S. R.; Collibee, S. E.; Agarkov, A. *J. Am. Chem. Soc.* **2000**, *122*, 6522. (i) Brauer, D. J.; Schenk, S.; Rossenbach, S.; Tepper, M.; Stelzer, O.; Häusler, T.; Sheldrick, W. S. *J. Organomet. Chem.* **2000**, *598*, 116. (j) Gilbertson, S. R.; Chang, C.-W. T. *J. Org. Chem.* **1998**, *63*, 8424. (k) Porte, A. M.; van der Donk, W. A.; Burgess, K. *J. Org. Chem.* **1998**, *63*, 5262. (l) Tepper, M.; Stelzer, O.; Häusler, T.; Sheldrick, W. S. *Tetrahedron Lett.* **1997**, *38*, 2257. (m) Gilbertson, S. R.; Chang, C.-W. T. *Chem. Commun.* **1997**, 975. (n) Gilbertson, S. R.; Pawlick, R. V. *Angew. Chem., Int. Ed. Engl.* **1996**, *35*, 902. (o) Gilbertson, S. R.; Wang, X. *J. Org. Chem.* **1996**, *61*, 434. (p) Gilbertson, S. R.; Starkey, G. W. *J. Org. Chem.* **1996**, *61*, 2922. (q) Gilbertson, S. R.; Chen, G.; McLoughlin, M. *J. Am. Chem. Soc.* **1994**, *114*, 4481.

(12) For the preparation of N-phosphino amino acids esters, see: Slawin, A. M. Z.; Woolins, D. J.; Zhang, Q. *J. Chem. Soc., Dalton Trans.* **2001**, 621.

(13) Selected examples: (a) Servin, P.; Laurent, R.; Romerosa, A.; Peruzzini, M.; Majoral, J.-P.; Caminade, A.-M. *Organometallics* **2008**, *27*, 2066. (b) Smoleński, P.; Pruchnik, F. P. *Pol. J. Chem.* **2007**, *81*, 1771. (c) Zhang, J.; Vittal, J. J.; Henderson, W.; Wheaton, J. R.; Hall, I. H.; Hor, T. S. A.; Yan, Y. K. *J. Organomet. Chem.* **2002**, *650*, 123. (d) Karasik, A. A.; Georgiev, I. O.; Musina, E. I.; Sinyashin, O. G.; Heinicke, J. *Polyhedron* **2001**, *20*, 3321. (e) Berning, D. E.; Katti, K. V.; Barnes, C. L.; Volkerts, W. A. *J. Am. Chem. Soc.* **1999**, *121*, 1658. (f) Kellner, K.; Hanke, W. *J. Organomet. Chem.* **1987**, *326*, C9. (g) Kellner, K.; Hanke, W.; Tzschach, A. *Z. Chem.* **1984**, *24*, 193. (h) Kellner, K.; Tzschach, A.; Nagy-Magos, Z.; Marko, L. *J. Organomet. Chem.* **1980**, *193*, 307. (i) Kostyanovskii, R. G.; El'natanov, Yu, I.; Shikhaliev, Sh. M. *Izv. Akad. Nauk. SSSR, Ser. Khim.* **1978**, 972.

(14) (a) Caprioara, M.; Fiammengo, R.; Engeser, M.; Jäschke, A. *Chem.−Eur. J.* **2007**, *13*, 2089 (phosphino-acyl amino acids and DNA). (b) Kobayashi, Y.; Tanaka, D.; Danjo, H.; Uozumi, Y. *Adv. Synth. Catal.* **2006**, *348*, 1561 (supported phosphine-acyl amino acid ligands). (c) Riondato, M.; Camporese, D.; Martín, D.; Suades, J.; Alvarez-Larena, A.; Mazzi, U. *Eur. J. Inorg. Chem.* **2005**, 4048 (phosphine-acyl glycine for radiopharmaceutical applications). (d) Breit, B.; Laungani, A. C. *Tetrahedron: Asymmetry* **2003**, *14*, 3823 (phosphino-acyl peptides). (e) Hird, A. W.; Hoveyda, A. H. *Angew. Chem., Int. Ed.* **2003**, *42*, 1276. (f) Lam, H.; Cheng, X.; Steed, J. W.; Aldous, D. J.; Hii, K. K. *Tetrahedron Lett.* **2002**, *43*, 5875 (chiral proline amidophosphines). (g) Gilbertson, S. R.; Chang, C.-W. T. *J. Org. Chem.* **1998**, *63*, 8424 (preparation of chiral oxazoline ligands). (h) Joó, F.; Trócsányi, E. *J. Organomet. Chem.* **1982**, *231*, 63 (Rh-catalyzed asymmetric hydrogenation with phosphinoacyl amino acid ligands). (i) Frolovskii, V. A.; Studnyev, Yu, N.; Rozancev, G. G. *Zh. Obshch. Khim.* **1993**, *63*, 1673 (condensation of $Ph_2P(O)CH_2CO_2Et$ with amino acids esters). See also ref 11a.

(15) For examples concerning amidation of ferrocene phosphinocarboxylic acids, see refs 6 and 8.

(16) Polášek, M.; Štěpnička, P. *J. Mass Spectrom.* **1998**, *33*, 739, and references therein.

Scheme 1. Synthesis of 1−6[a]

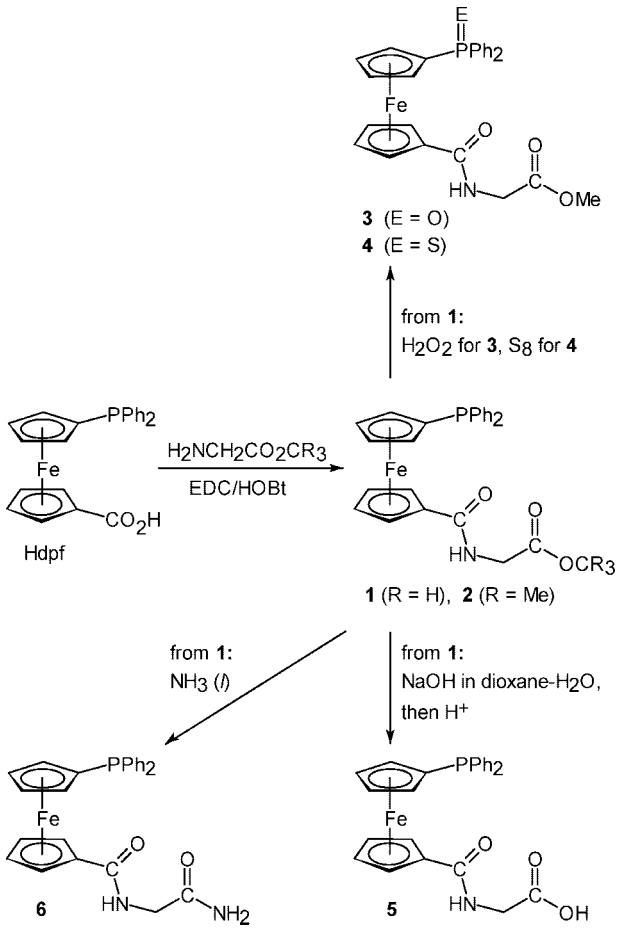

[a] HOBt = 1-hydroxybenzotriazole, EDC = *N*-[3-(dimethylamino)-propyl]-*N*′-ethylcarbodiimide.

characterized similarly to their parent amide **1**, and the solid-state structures of **3**, **4**, and **6** were established by X-ray crystallography.

Modifications of the phosphorus substituent (**1** → **3** and **4**) are clearly reflected in the ^{31}P NMR spectra through a shift to lower fields (δ_P = 32.1 for **3** and 42.9 for **4**). The position of the ^{31}P signals as well as the ^{1}H and ^{13}C NMR parameters of the $Ph_2P(E)$-substituted ferrocenyl groups (E = O and S) match those of the respective Hdpf derivatives,[3,6f] whereas the NMR response of glycine pendant group in **3** and **4** remain largely unaffected. On the other hand, modifications at the glycine moiety such as in **5** and **6** have quite opposite (though not dramatic) effect. The carboxyl $\nu_{C=O}$ band in the IR spectrum of **5** is shifted to lower energies than for **1**, while the amide bands appear moved in the opposite direction. The IR spectra of **6** and **1** differ expectedly more because of the change at the polar functional moiety (CO_2Me → $C(O)NH_2$).

Crystal Structures of 2−4 and 6. The molecular structures of **2**, **3**, **4**, and **6** are shown in Figures 1−4. Relevant geometric data are given in Table 1. The overall molecular geometries compare favorably with those of Hdpf,[3] its P-chalcogen derivatives,[3,6f] and the related ferrocenecarboxylic derivatives: $FcCONHCH_2CO_2R$ (R = Me and CH_2Ph;[17] Fc = ferrocenyl) and $fc(CONHCH_2CONH_2)_2 \cdot 2H_2O$ (fc = ferrocene-1,1′-diyl).[18]

The ferrocene units in **2**−**4** and **6** are regular, showing negligible tilts and similar Fe−ring centroid distances. The secondary amide moieties are planar but tilted with respect to their parent cyclopentadienyl (Cp) rings (see φ angles in Table 1). Additional differences can be seen in the conformation at the N−C(24) bond and, particularly, in the mutual orientation of the ferrocene substituents (Table 1). The substituents in **2** assume a conformation close to anti-eclipsed (ideal value τ = 144°), whereas those in **3** and **4** are near to syn-eclipsed (ideal value 72°). This is apparently due to the formation of intramolecular N−H···E hydrogen bonds in the chalcogenides (E = O for **3** and S for **4**; Table 2), the longer E···N distance in **4** corresponding with the higher τ and lower φ angles. Apart from this interaction, the molecules of **3** and **4** generate similar sets of soft intra- and intermolecular C−H···E contacts in their crystals (Table 2) that, when taken together, lead to the formation of centrosymmetric dimer units and their columnar propagation (Figure 2b).

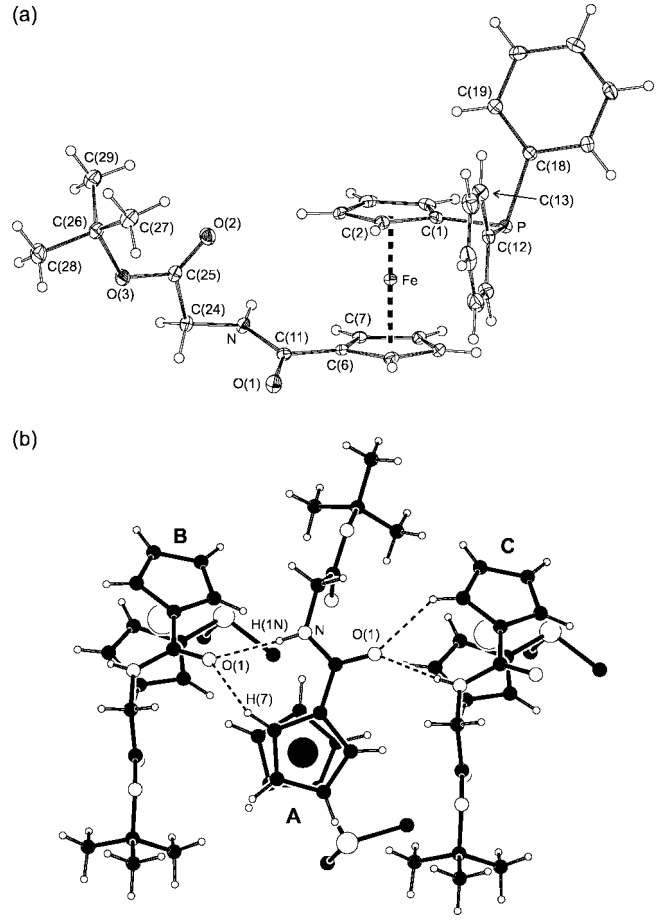

Figure 1. (a) View of the molecular structure of **2** showing displacement ellipsoids at the 30% probability level and the atom-labeling scheme. (b) Depiction of intermolecular H-bond interactions in the structure of **2**. Only pivotal atoms from the phenyl rings are shown for clarity. Symmetry operations: $A = (x, y, z)$, $B = (x, 1/2-y, -1/2+z)$, $C = (x, 1/2-y, 1/2+z)$.

The ferrocene moiety in **6** adopts a conformation near to syn-eclipsed (i.e., similar to **4**), but the C(11)−N−C(24)−C(25) angle is more opened. Such changes are in accordance with intermolecular aggregation, which is more complex than in **2**−**4** owing to a higher number of available H-bond donors. Individual molecules of **6** assemble to centrosymmetric dimers via N(2)−H(3N)···O(1) hydrogen bonds. These dimers further associate through N−H···O interactions, forming layers parallel to the crystallographic *bc* plane (Figure 5, Table 2). Softer C−H···O contacts support the formed assembly.

Preparation and Structural Characterization of Bis-phosphine Complexes 7−9. Reactions of $[PdCl_2(cod)]$ (cod = η^2:η^2-cycloocta-1,5-diene) with **1** and **6** and the reaction of

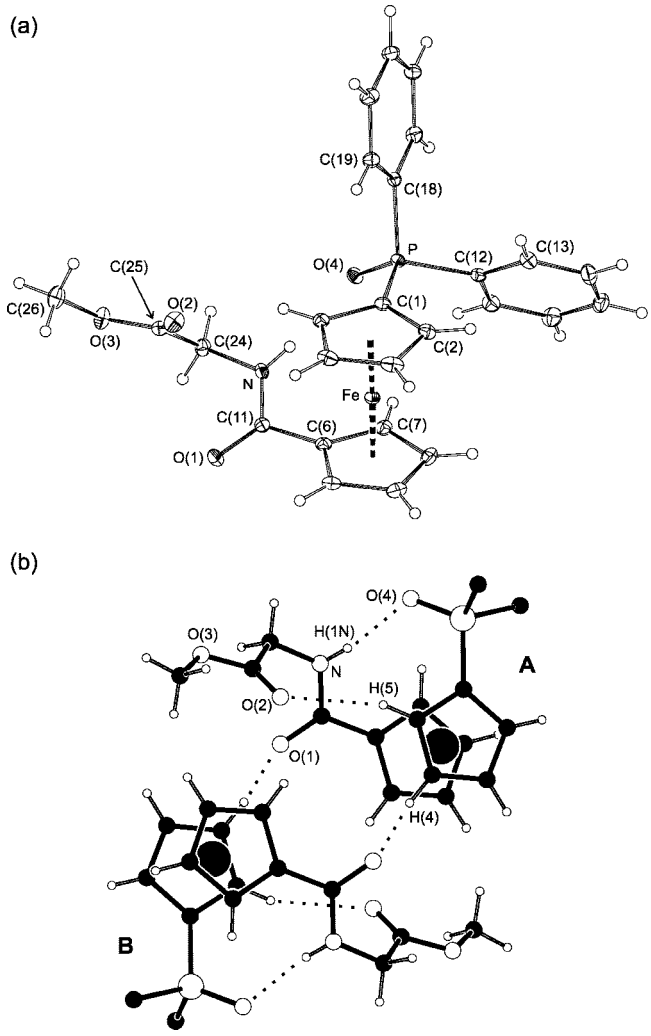

Figure 2. (a) Molecular structure of **3**. Displacement ellipsoids correspond to 30% probability. (b) View of the dimeric motif in the crystal of **3** showing hydrogen bonds as dotted lines. Phenyl ring carbon atoms are omitted for clarity. Molecules A and B relate by a crystallographic inversion operation.

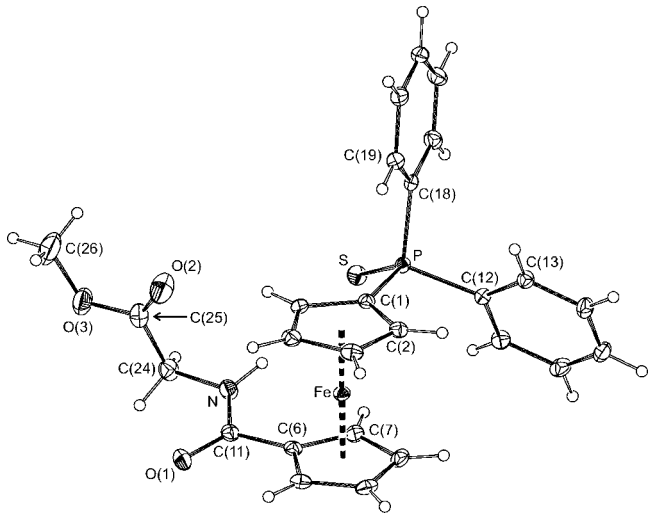

Figure 3. Molecular structure of **4**. Displacement ellipsoids are drawn at the 30% probability level.

$Na_2[PdCl_4]$ with **5** proceed straightforwardly to yield bis-phosphine complexes **7**−**9** (Scheme 2). Complex **7** was isolated solvent-free, while its more polar analogues **8** and **9** resulted as

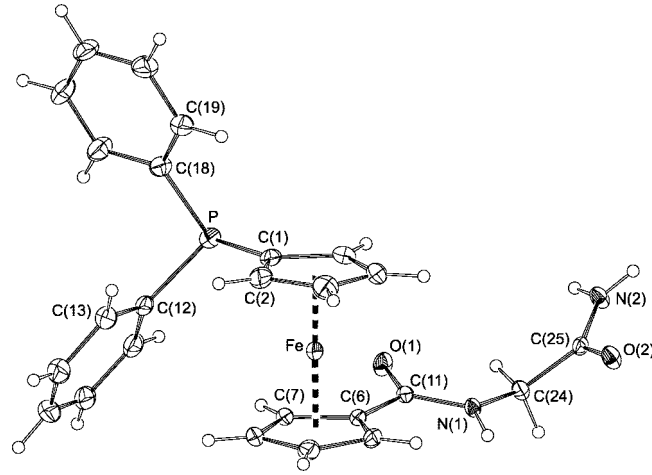

Figure 4. Molecular structure of diamide **6**. Displacement ellipsoids correspond to the 30% probability level.

Table 1. Selected Distances and Angles for 2−4 and 6 (in Å and deg)[a]

parameter	2	3	4	6
E	void	O(4)	S	void
Fe−Cg(1)	1.6521(7)	1.6385(8)	1.6480(7)	1.645(1)
Fe−Cg(2)	1.6489(7)	1.6451(7)	1.6536(7)	1.648(1)
∠Cp(1),Cp(2)	0.33(9)	2.14(9)	1.96(9)	2.1(2)
τ^b	133	74	86	89
P═E		1.494(1)	1.9601(4)	
C(11)−O(1)	1.235(2)	1.225(2)	1.230(2)	1.229(3)
C(11)−N	1.349(2)	1.348(2)	1.351(2)	1.353(3)[d]
N−C(24)	1.445(2)	1.438(2)	1.443(2)	1.450(3)[d]
C(25)−O(2)	1.202(2)	1.193(2)	1.196(2)	1.243(3)
C(25)−O(3)	1.339(2)	1.342(2)	1.340(2)	1.321(3)[e]
O(3)−C(26)	1.492(2)	1.446(2)	1.452(3)	
φ^c	26.1(2)	26.7(2)	14.9(2)	13.6(3)
O(1)−C(11)−N	121.8(1)	122.5(1)	122.5(1)	122.1(2)[d]
C(11)−N−C(24)	121.5(1)	118.7(1)	120.2(1)	119.7(2)[d]
O(2)−C(25)−O(3)	126.1(1)	124.5(1)	124.0(2)	122.6(2)[f]
C(25)−O(3)−C(26)	121.4(1)	115.4(1)	115.9(2)	
O(1)−C(11)−N−C(24)	5.6(2)	7.9(2)	4.9(2)	4.4(3)[d]
C(11)−N−C(24)−C(25)	92.9(2)	65.2(2)	87.2(2)	126.9(2)[d]

[a] The ring planes are defined as follows: Cp(1) = C(1−5), Cp(2) = C(6−10). Cg(1) and Cg(2) denote the respective ring centroids. [b] Torsion angle C(1)−Cg(1)−Cg(2)−C(6). [c] Dihedral angle of the Cp(2) and {C(11), O(1), N} ({C(11), O(1), N(1)} for **6**) planes. [d] Parameter involving N(1). [e] C(25)−N(2). [f] O(2)−C(25)−N(2).

stoichiometric solvates with three water and four acetic acid molecules per the complex molecule, respectively. Yet another solvate, *trans*-$[PdCl_2(\mathbf{6}\text{-}\kappa P)_2]\cdot 4CHCl_3$ (**9a**), was obtained upon crystallization of **9** from chloroform/hexanes.

Complexes **7**−**9** were characterized by elemental analysis and by NMR, IR, and ESI mass spectra; a negligible solubility of **8** precluded any NMR analysis.[19] ^1H and ^{31}P NMR data of **7** and **9** indicate that the ferrocene ligands are chemically equivalent and coordinate as monodentate phosphines, the ^{31}P NMR data comparing well with those of *trans*-$[PdCl_2(Hdpf\text{-}\kappa P)_2]$.[20] The P-monodentate coordination was corroborated by IR spectra, showing the amide bands at positions similar to the free ligands. In addition, the ^{13}C NMR spectra exhibited signals due to the

(17) (a) Gallagher, J. F.; Kenny, P. T. M.; Sheehy, M. J. *Inorg. Chem. Commun.* **1999**, *2*, 200. (b) Gallagher, J. F.; Kenny, P. T. M.; Sheehy, M. J. *Acta Crystallogr, Sect. C, Cryst. Struct. Commun.* **1999**, *55*, 1257.

(18) Georgopoulou, A. S.; Mingos, D. M. P.; White, A. J. P.; Williams, D. J.; Horrocks, B. R.; Houlton, A. *J. Chem. Soc., Dalton Trans.* **2000**, 2969.

(19) Complex **8** is virtually insoluble in all common laboratory solvents except for warm dimethylsulfoxide, in which, however, it rapidly decomposes.

Table 2. Hydrogen Bond Parameters for the Structures of 2−4 and 6[a]

D−H···A	D···A (Å)	D−H···A (deg)
Compound **2**		
N(1)−H(1N)···O(1^{i})	2.953(2)	171(2)
C(7)−H(7)···O(1^{i})	3.058(2)	135
C(3)−H(3)···O(2) (I)	3.365(2)	163
Compound **3**		
N(1)−H(1N)···O(4) (I)	2.858(2)	172(2)
C(5)−H(5)···O(2) (I)	3.413(2)	158
C(4)−H(4)···O(1^{ii})	3.322(2)	150
C(26)−H(26C)···O(1^{iii})	3.114(2)	126
Compound **4**		
N(1)−H(1N)···S (I)	3.659(1)	176
C(2)−H(2)···O(2) (I)	3.456(2)	160
C(16)−H(16)···O(1^{iv})	3.477(2)	160
C(20)−H(20)···O(1^{v})	3.337(2)	155
Compound **6**		
N(1)−H(1N)···O(2^{vi})	3.149(2)	175
N(2)−H(2N)···O(2^{vii})	2.877(3)	175
N(2)−H(3N)···O(1^{viii})	2.846(3)	166
C(10)−H(10)···O(2^{vi})	3.315(3)	137
C(24)−H(24A)···O(1^{viii})	3.281(3)	147

[a] Legend: D = donor, A = acceptor, (I) = intramolecular contact. Symmetry codes: i (x, 1/2−y, −1/2+z), ii (1−x, −1−y, 1−z), iii (1−x, 1/2+y, 3/2−z), iv (1−x, 1−y, 1−z), v (x, 3/2−y, −1/2+z), vi (1−x, 1/2+y, 1/2−z), vii (1−x, −1/2+y, 1/2−z), viii (1−x, −y, 1−z).

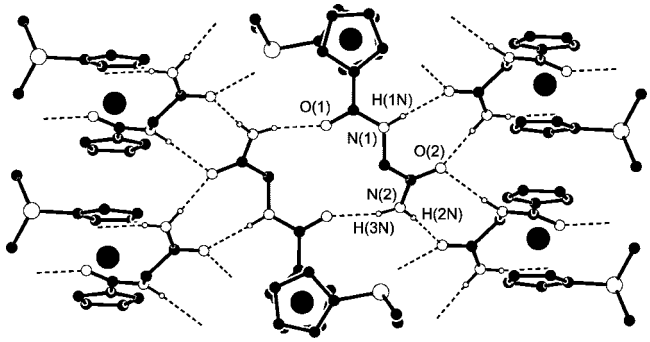

Figure 5. Section of the solid-state molecular assembly of **6** showing hydrogen bonds as dashed lines. Phenyl ring carbons and CH hydrogens are omitted to avoid complicating the figure.

Scheme 2. Synthesis of Bis-phosphine Complexes 7−9

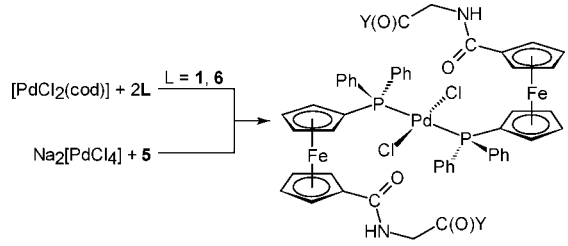

7 (L = **1**, Y = OMe)
8 (L = **5**, Y = OH)
9 (L = **6**, Y = NH_2)

phosphinylated Cp and phenyl ring carbons (CH and C_{ipso}, except for phenyl CH_{para}) as apparent triplets. Such behavior is typical for ABX spin systems $^{12}C-^{31}P(A)-M-^{31}P(B)-^{13}C(X)$ (M = metal)[21] arising in bis-phosphine complexes and was

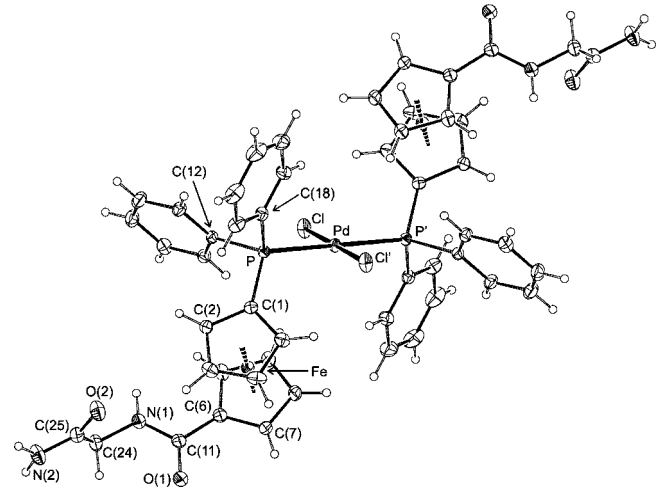

Figure 6. View of the complex molecule in the crystals of **9**. Displacement ellipsoids enclose 30% probability. Primed atoms are generated by the crystallographic inversion.

Table 3. Comparison of the Selected Structural Data for 9 and 9a (values in Å and deg)[a]

parameter	**9**	**9a**
Pd−Cl	2.2955(9)	2.283(1)
Pd−P	2.3374(8)	2.3522(9)
Cl−Pd−P[b]	93.67(3)	90.40(4)
Fe−Cg(1)	1.645(2)	1.641(2)
Fe−Cg(2)	1.647(2)	1.640(2)
∠Cp(1),Cp(2)	3.5(2)	1.3(3)
C(11)−O(1)	1.239(5)	1.239(5)
C(11)−N(1)	1.339(5)	1.338(5)
O(1)−C(11)−N(1)	120.8(3)	121.6(4)
C(25)−O(2)	1.240(4)	1.226(6)
C(25)−N(2)	1.318(5)	1.324(6)
O(2)−C(25)−N(2)	124.0(4)	123.3(4)
τ[c]	138	151
φ[d]	6.8(4)	14.8(5)
O(1)−C(11)−N(1)−C(24)	2.4(5)	4.5(6)
C(11)−N(1)−C(24)−C(25)	88.6(4)	83.9(5)

[a] The ring planes are defined as follows: Cp(1) = C(1−5), Cp(2) = C(6−10). Cg(1) and Cg(2) denote the respective ring centroids. [b] The Cl−Pd−P and Cl−Pd−P′ angles sum up to 180° due to molecular symmetry. [c] Torsion angle C(1)−Cg(1)−Cg(2)−C(6). [d] Dihedral angle of the Cp(2) and {C(11), O(1), N(1)} least-squares planes.

previously noted for the related complexes *trans*-[$PdCl_2$(Ph_2PfcY-κP)$_2$] (Y = CO_2H,[20] CH=CH_2,[22] and PO_3Et_2[23]).

Crystal structures of **9** and **9a** have been determined in order to establish the influence of the solvent of crystallization on the crystal assembly. The molecular structure of **9** is shown in Figure 6 (for structural drawings of **9** and **9a**, see Supporting Information, Figure S1). Geometric data for **9** and **9a** are presented in Table 3.

Both solvatomorphs crystallize with the symmetry of the $P\bar{1}$ space group, with the Pd atoms residing on crystallographic inversion centers. This renders only half of their molecules structurally independent and makes the coordination environment around palladium perfectly planar. Owing to the imposed symmetry, the "PC_3" moieties are staggered and the ferrocene ligands assume anti positions. Whereas the Pd−Cl/P distances and Cl−Pd−P/P′ angles in **9** are almost identical with those found for *trans*-[$PdCl_2$(Hdpf-κP)$_2$]·2AcOH,[20] the parameters

(20) Štěpnička, P.; Podlaha, J.; Gyepes, R.; Polášek, M. *J. Organomet. Chem.* **1998**, *552*, 293.

(21) Pregosin, P. S.; Kunz, R. W. *^{31}P and ^{13}C NMR of Transition Metal Phosphane Complexes in NMR Basic Principles and Progress*; Diehl, P., Fluck, E., Kosfeld, R., Eds.; Vol. 16, Chapter E, pp 65ff, and references therein.

(22) Štěpnička, P.; Císařová, I. *Collect. Czech. Chem. Commun.* **2006**, *71*, 215.

(23) Štěpnička, P.; Císařová, I.; Gyepes, R. *Eur. J. Inorg. Chem.* **2006**, 926.

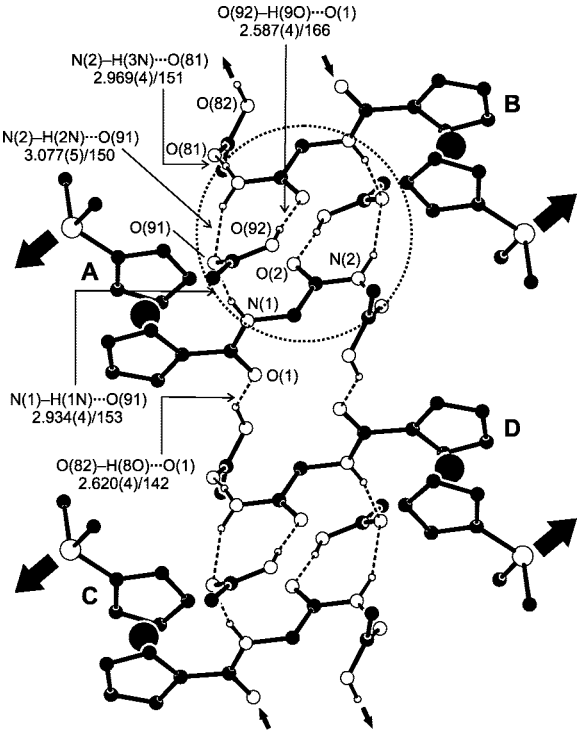

Figure 7. Section of the H-bonded array in solid **9**. Hydrogen bonds are shown as dashed lines, and the hydrogen-bonded cage is highlighted with a dotted circle. Propagation of the supramolecular assembly is indicated with small (via H-bonds) and larger (via $PdCl_2$) arrows. For clarity, phenyl ring carbons, irrelevant hydrogens, and $PdCl_2$ units are omitted. Data for H-bonds are given as follows: D−H···A, D···A (Å)/D−H···A angle (deg) (D = donor, A = acceptor). Molecules A and B (C and D) relate by crystallographic inversion; the C−D pair results by translation of A−B along the *b* axis.

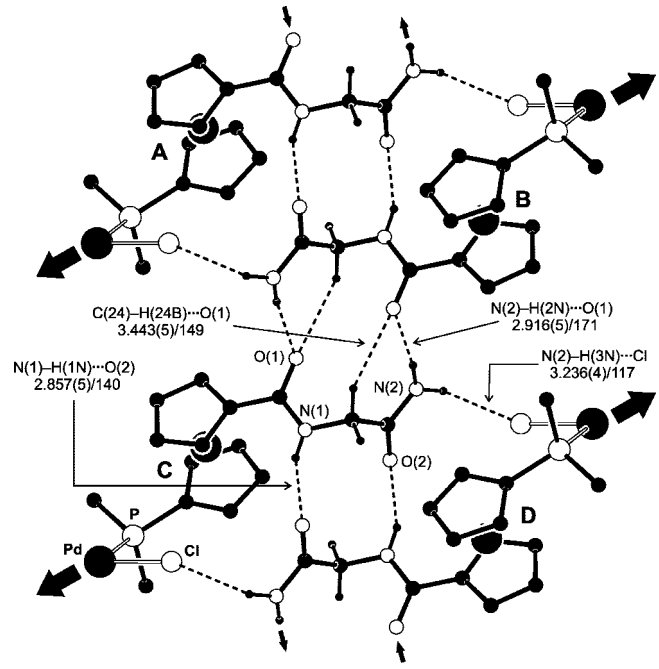

Figure 8. Section of the H-bonded array in the crystal of **9a** showing hydrogen bonds as dashed lines. For clarity, phenyl ring carbons, irrelevant hydrogens, and solvating molecules are omitted. Propagation of the assembly is indicated with small (via H-bonds) and larger (via $PdCl_2$ moieties) arrows. H-bond parameters are given as for **9** (see caption to Figure 7). Molecules A and B (C and D) relate by crystallographic inversion; molecules C and D result by translation of A and B along the *a* axis.

of **9a** slightly differ from **9** and the reference compound (*N.B.* The interligand angles in **9a** deviate from the ideal 90° only negligibly). Another difference can be found in the mutual orientation of the ferrocene ligands and the coordination plane, the dihedral angles of the Cp(1) and {Pd,Cl,P} planes being 52.2(2)° and 36.1(2)° for **9** and **9a**, respectively. Compared to free **6**, the ferrocene substituents in **9** and **9a** are more distant, assuming positions near anti-eclipsed (Figure S1). The Cp-bound amide moiety {C(11),O(1),N(1)} in **9a** is symmetrically rotated around the C(6)−C(11) bond ($\varphi \approx 15°$). In **9** the amide plane exerts a lower rotation but is tilted toward the ferrocene unit.[24] The conformation of the glycine pendants is changed as well, reflecting hydrogen bond formation (Table 3).

As expected, the crystal architecture of both **9** and **9a** is based on hydrogen-bonding interactions. In the crystals of **9**, the *ligand units* and the solvent assemble into centrosymmetric cages by means of N−H···O and O−H···O hydrogen bonds (Figure 7). These cages are interlinked via H-bonds generated by the second acetic acid molecule, forming columnar stacks oriented parallel to the crystallographic *b* axis. However, since each complex molecule possesses *two* ligands, these stacks propagate into infinite layers through the $PdCl_2$ fragments. Additional intermolecular C−H···O and C−H···Cl contacts cross-link the individual sheets.

On the other hand, the *ligands* in **9a** aggregate into ladder-like arrays oriented along the crystallographic *a* axis via cooperative N−H···O/Cl and C−H···O interactions (Figure 8).[25] Further propagation of the molecular assembly again occurs via the $PdCl_2$ moiety, giving rise to sheets in the crystallographic *ac* plane. Unlike **9**, however, these sheets are not interconnected but instead define structural voids that host the solvent of crystallization.[26]

Synthesis and Crystal Structures of (L^{NC})Pd Complexes. Three chemically different palladium(II) complexes with a 2-[(dimethylamino-κN)methyl]phenyl-κC^1 (L^{NC}) auxiliary ligand, compounds **10**−**12**, have been prepared from ligand **1** (Scheme 3). First, a bridge cleavage reaction between dimer [{Pd(μ-Cl)(L^{NC})}$_2$] and **1** cleanly afforded complex **10** in 95% yield after crystallization. Subsequent halide removal with $AgClO_4$ yielded cationic complex **11** (90% yield), in which the amide oxygen takes up the free coordination site with concomitant closure of a P,O-chelate ring. Another bis-chelate complex **12** resulted when **10** was treated with potassium *tert*-butoxide (59% yield after crystallization). The conversion of **10** into **12** formally consists of two steps: the removal of the amide proton with *t*-BuO^- and the intramolecular displacement of the Pd-bound chloride, converting the ferrocene ligand to an anionic P,N-chelate donor. The reverse reaction also proved feasible, complex **12** being smoothly converted back to **10** upon treatment with 1 molar equiv of HCl.

Complexes **10**−**12** were characterized by spectral methods and by elemental analysis, and their solid-state structures were

(24) The distances from the Cp(2) plane for **9**/**9a** are as follows: C(11) 0.109(4)/0.012(4), O(1) 0.034(3)/−0.275(3), and N(1) 0.268(3)/0.295(4) Å.

(25) The H-bond parameters are as follows: C(15)−H(15)···O(92): C(15)···O(92) = 3.272(5) Å, angle at H(15) = 149°; C(20)−H(20)···Cl: C(20)···Cl = 3.673(4) Å; angle at H(20) = 155°; C(24)−H(24A)···O(1): C(24)···O(1) = 3.384(5) Å, angle at H(24A) = 144°.

(26) The solvate molecules form Cl_3C−H···O contacts to carbonyl oxygens of the ligand. The H-bond parameters are as follows: C(80)−H(80)···O(2): C(80)···O(2) = 3.056(6) Å; angle at H(80) = 163°; C(90)−H(90)···O(1): C(90)···O(1) = 3.111(7) Å; angle at H(90) = 164°.

Scheme 3. Preparation and Reactions of (L^{NC})Pd Complexes with Ligand 1

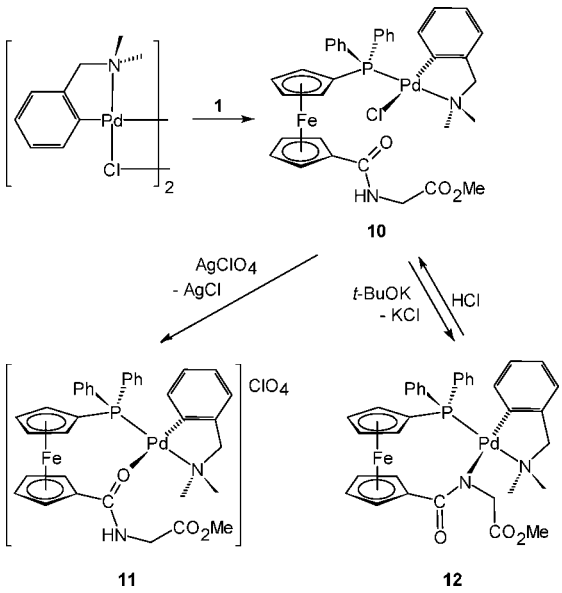

established by single-crystal X-ray diffraction analysis. NMR spectra of **10**−**12** reveal characteristic signal sets attributable to L^{NC} and the ferrocene ligands. The NMR data correspond with those reported for Pd(L^{NC}) complexes with phosphinocarboxylic donors[27] and, via the $^3J_{PC}$ and $^4J_{PC}$ coupling constants, suggest a *trans*-P,N relationship[27] in all cases. The ^{31}P NMR signals are found in a rather narrow range, δ_P 30.9−33.6 (**12** > **10** > **11**), shifted downfield versus free **1**. The ^{1}H and ^{13}C NMR parameters of **10**−**12** are roughly similar (especially those relating to molecular parts not involved in coordination). It should be noted, however, that despite the planar chirality resulting from fixed conformation of the ferrocene unit in the bis-chelate complexes, the resonances due to ferrocene CH groups are observed as nondegenerate only for **12** (eight diastereotopic signals). This may reflect a lower flexibility of the anionic (P,N$^-$) chelate over the neutral (P,O) one. Structural data support this explanation.

Conversion of **10** into **11** causes relatively small changes in the NMR parameters. The most notable change is observed for the amide C═O group, the C-13 resonance of which shifts from ca. δ_C 170−171 (in **10**) to δ_C 175.27. Deprotonation and coordination of the amide nitrogen (**10** → **12**) has a more pronounced effect: The ^{1}H NMR signals due to glycine CH_2 protons in **12** become anisochronic ($\Delta\delta_H$ = 0.48), but their average chemical shift (δ_H 4.06) remains nearly the same as in **10** and **11**. The C-13 signals due to the glycine moiety in **12** are shifted significantly more (CH_2 by +9.8 ppm and the amide C═O by ca. +4 ppm vs **10**). Finally, a resonance due to the amide proton is expectedly missing from the ^{1}H NMR spectrum of **12**, and one of the ferrocene signals (α-CH at the amide-substituted Cp ring) appears markedly downfield compared to the remaining ones (δ_H 6.44 vs 4.09−4.91).

Because complexes **10**−**12** differ predominantly at their polar pendants, valuable structural information can be inferred from their IR spectra. Upon converting **10** to **11**, the ν_{NH} band moves to higher energies, the frequency of the amide I band ($\nu_{C=O}$) decreases by ca. 30 cm^{-1}, while that of the amide II band (largely NH bending) increases by 35 cm^{-1}. The ester $\nu_{C=O}$ band also shifts to higher frequencies, albeit much less. Furthermore, the IR spectrum of **11** also confirms the presence of the perchlorate counterion. The conversion of **10** to **12** is reflected by a disappearance of the ν_{NH} band and a shift of the amide I and ester $\nu_{C=O}$ bands to lower energies (by ca. 60 and 20 cm^{-1} vs **10**, respectively).

Views of the molecular structures of **10**−**12** are presented in Figure 9, and selected geometric data are given in Table 4. Unlike **11**, complexes **10** and **12** crystallize with two molecules in the asymmetric unit. The structurally independent molecules of **10** are very similar (see Supporting Information, Figure S2), and their multiplication likely results from intermolecular interactions.[28] On the other hand, the molecules of **12** differ substantially (Table 4, Figure S2), and the reasons for their duplication in the asymmetric unit remain unclear.

Generally, the structural parameters of **10**−**12** compare well with the data reported for (L^{NC})Pd complexes featuring simple and ferrocene-based phosphinocarboxylic ligands[27,29] and confirm a *trans* P−N(metallacycle) relation as suggested from NMR data. The coordination environment around the palladium atoms in **10**−**12** departs significantly from the regular square owing to different Pd−donor bond lengths, steric constraints imposed by the small palladacycle, and limitations resulting from spatial contacts between the ligands.[30] Whereas the Pd−P and Pd−C bonds in **10**−**12** are of similar length, all other Pd−donor distances differ noticeably, even among the structurally independent molecules. Likewise, the N−Pd−C angle within the rigid metallacycle varies only by ca. 1.5° (ring puckering parameters confirm structural similarity of the (L^{NC})Pd units;[31] Table 4), while all other interligand angles change significantly more.

Interatomic distances and angles within the ferrocene ligands are similar to those of free ester-amide **2**; notable differences are seen in the conformation. The P-monodentate ligand in **10** has the sterically relaxed anti-eclipsed conformation, and its carboxamide moiety is coplanar with its parent Cp(2) ring ($\varphi \approx 2°$). Formation of chelate rings in **11** and **12** requires reorientation of the ferrocene substituents to a conformation close to syn-eclipsed (τ: **12** < **11** < ideal value 72°) and, simultaneously, leads to distortion of the carboxamide moiety. As evidenced by the φ angles, the amide planes in the chelate complexes are no longer coplanar with their bonding Cp(2) plane (φ: **12** > **11** ≫ **10**) because the amide donor atoms are brought to proximity of Pd via a combination of symmetric rotation along the pivotal C(Cp)−C bond and twisting of the C(O)N

(27) Ferrocene-based ligands: (a) Štěpnička, P.; Lamač, M.; Císařová, I. *Polyhedron* **2004**, *23*, 921. (b) Štěpnička, P. *Inorg. Chem. Commun.* **2004**, *7*, 426. (c) Štěpnička, P.; Císařová, I. *Organometallics* **2003**, *22*, 1728. See also ref 5e. "Simple" phosphinocarboxylic ligands: (d) Braunstein, P.; Matt, D.; Dusausoy, Y.; Fischer, J.; Mitschler, A.; Ricard, L. *J. Am. Chem. Soc.* **1981**, *103*, 5115. (e) Braunstein, P.; Matt, D.; Nobel, D.; Bouaoud, S.-E.; Grandjean, D. *J. Organomet. Chem.* **1986**, *301*, 401.

(28) The molecules of **10** form infinite chains along the *b* direction via N−H···Cl contacts between alternating, structurally independent moieties 1 and 2. The H-bond parameters are as follows (without symmetry codes): N(11)−H(1N)···Cl(2): N(11)···Cl(2) = 3.249(3) Å, angle at H(1N) = 155°; N(21)−H(2N)···Cl(1): N(21)···Cl(1) = 3.194(3) Å, angle at H(2N) = 150°. These chains are interconnected by C−H···O contacts.

(29) Structural data for some related compounds can be found in: (a) Štěpnička, P.; Císařová, I. *Inorg. Chem.* **2006**, *45*, 8785. (b) Ma, J.-F.; Yamamoto, Y. *Inorg. Chim. Acta* **2000**, *299*, 164. See also ref 22.

(30) The maximum deviations from the least-squares planes comprising the palladium and its four ligating atoms are ca. 0.10/0.14 Å for **10** (molecule 1/2), ca. 0.19 Å for **11**, and ca. 0.12/0.11 Å for **12** (molecule 1/2).

(31) Although any ring puckering analysis for the palladacycles can be regarded as dubious due to very different in-ring bond lengths, the parameters describe the *same* moiety and their trend is unambiguous. For a reference, see: Cremer, D.; Pople, J. A. *J. Am. Chem. Soc.* **1975**, *97*, 1354.

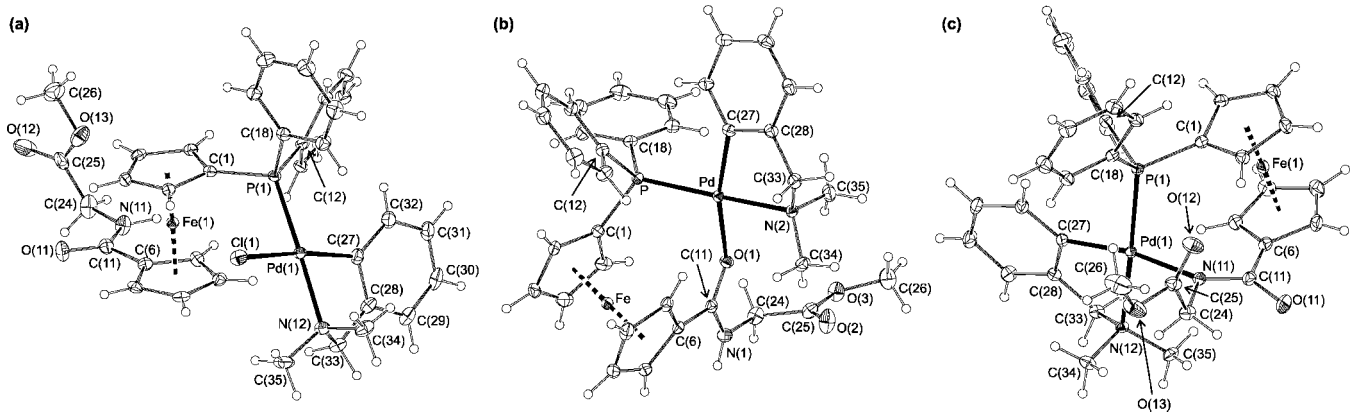

Figure 9. Molecular structures of **10**−**12**: (a) molecule 1 in the structure of **10**, (b) cation in the structure of **11**, and (c) molecule 1 in the structure of **12**. Displacement ellipsoids enclose 30% probability. Note: Atom labels in molecules 2 are obtained by changing the first digit in the respective label to 2 for heavy atoms (except for C) and by adding 40 (for **10**) or 50 (for **12**) for the carbon atom labels.

Table 4. Selected Distances and Angles for Complexes 10−12 (in Å and deg)[a]

	10 (E = Cl)			**12** (E = N(11)/N(21))	
parameter	molecule 1	molecule 2	**11** (E = O(1))	molecule 1	molecule 2
Pd−E	2.4123(9)	2.4120(9)	2.145(1)	2.127(2)	2.109(2)
Pd−P	2.266(1)	2.262(1)	2.2569(6)	2.2597(5)	2.2644(5)
Pd−N	2.144(3)	2.161(3)	2.145(2)	2.188(2)	2.166(2)
Pd−C	2.018(4)	2.015(4)	1.998(2)	2.025(2)	2.028(2)
E−Pd−P	90.86(3)	90.94(3)	98.43(4)	96.30(5)	88.34(5)
E−Pd−N	91.70(8)	91.57(8)	87.50(6)	90.06(7)	92.01(7)
P−Pd−C	97.0(1)	97.1(1)	92.92(6)	93.19(6)	98.57(6)
N−Pd−C	80.8(1)	81.2(1)	82.50(8)	80.96(8)	81.49(8)
Q_{ring}[b]	0.498(3)	0.452(3)	0.429(2)	0.508(2)	0.427(2)
φ_{ring}[b]	30.7(4)	212.05(5)	221.6(3)	213.0(2)	220.4(4)
Fe−Cg(1)	1.648(2)	1.648(2)	1.644(1)	1.640(1)	1.642(1)
Fe−Cg(2)	1.652(2)	1.647(2)	1.647(1)	1.647(1)	1.642(1)
∠Cp(1),Cp(2)	3.0(2)	2.9(2)	6.5(1)	6.9(1)	8.4(1)
τ[c]	148	149	61	58	53
φ[d]	2.0(4)	2.3(4)	19.8(2)	24.5(3)	21.9(3)
C═O[e]	1.228(5)	1.237(5)	1.252(2)	1.253(3)	1.252(3)
C−N[e]	1.341(5)	1.353(5)	1.334(3)	1.341(3)	1.332(3)
N−C═O[e]	122.5(4)	121.9(4)	119.3(2)	125.4(2)	123.6(2)
C(OMe)═O[f]	1.201(6)	1.195(6)	1.193(3)	1.197(3)	1.202(3)
(O)C−OMe[f]	1.309(6)	1.345(6)	1.330(3)	1.346(3)	1.341(3)

[a] The ring planes are defined as follows: Cp(1) = C(1−5), Cp(2) = C(6−10). Cg(1) and Cg(2) stand for the respective ring centroids. Labeling of "molecules 2" is strictly analogous (see comment in Figure 9). [b] Ring puckering parameters: Q_{ring} = total puckering amplitude, φ_{ring} = phase angle. Ideal envelope requires φ_{ring} to be equal to $k \times 36°$ (i.e., 36° or 216° in the present cases). See ref 31. [c] Torsion angle C(1)−Cg(1)−Cg(2)−C(6). [d] Dihedral angle of the Cp(2) and its bonded {C,O,N} plane. [e] Parameters describing the Cp-bound amide moiety. [f] Parameters involving the terminal methoxycarboxyl group.

unit.[32] Coordination of the amide moiety in either form (neutral via O or deprotonated via N) brings on a slight elongation of the C═O bond (ca. 0.02 Å) and an even less pronounced shortening of the C−N bond (on average). The data in Table 4 indicate that the deformation of the ligand structure increases from **10** to **11** and further to **12**: first markedly, owing to chelate formation, and then less due to steric crowding when the glycine pendant is forced closer to the coordination plane and to other ligands.

Electrochemistry. Electrochemical behavior of Gly-amides (**1**, **3**−**6**) and of complexes **10**−**12** was studied by cyclic voltammetry (CV) at a platinum disk electrode on dichloromethane solutions. The pertinent data are summarized in Table 5.[33,34]

Table 5. Summary of Electrochemical Data[a]

compound	wave I: $E^{\circ\prime}$ [V]	further waves: E_{pa}/E_{pc} [V]
1	0.26	0.40/0.31, 0.86/- (II)
3	0.43	n.o.
4	0.43	$E_{pa} > 1.0$ V (II)
5	$E_{pa} = 0.30$	0.85/− (II)
6	$E_{pa} = 0.29$	0.77/0.63 (II)
10	0.32	0.63/0.55, ca. 0.93 (E_{pa}, II)
11	0.59	n.o.
12	0.21	ca. 0.22, 0.48, 0.62 (all E_{pa})

[a] See text for discussion. Recorded at platinum electrode in dichloromethane solutions. The potentials are given relative to the ferrocene/ferrocenium couple. For details, see Experimental Part. $E^{\circ\prime} = 1/2(E_{pa} + E_{pc})$, where E_{pa} (E_{pc}) is the anodic (cathodic) peak potential in CV. n.o. = not observed.

Ester-amide **1** undergoes an oxidation (wave I, Figure 10, A), which is electrochemically quasi-reversible when scanned separately ($E^{\circ\prime} = 0.26$ V, $\Delta E_p = 90$ mV at scan rate 100 mV s^{-1}) and can be attributed to a ferrocene/ferrocenium couple. Its shift toward more positive potentials versus ferrocene itself (but negative of Hdpf: $E^{\circ\prime} = 0.32$ V[3]) corresponds with the nature of the substitutens (cf. σ_P constants:[35] 0.36 for $CONH_2$

(32) The distances of the C/O/N atoms forming the amide plane from the Cp(2) plane are as follows (in Å): **10**: 0.054(4)/0.093(3)/0.047(3) and [0.021(4)/0.063(3)/0.027(3)] for molecule 1 [molecule 2]; **11**: 0.241(2)/0.665(1)/0.025(2); **12**: 0.119(2)/0.278(2)/0.657(2) [0.271(2)/0.125(2)/0.751(2)] for molecule 1 [molecule 2]. Directions of the displacement are not indicated.

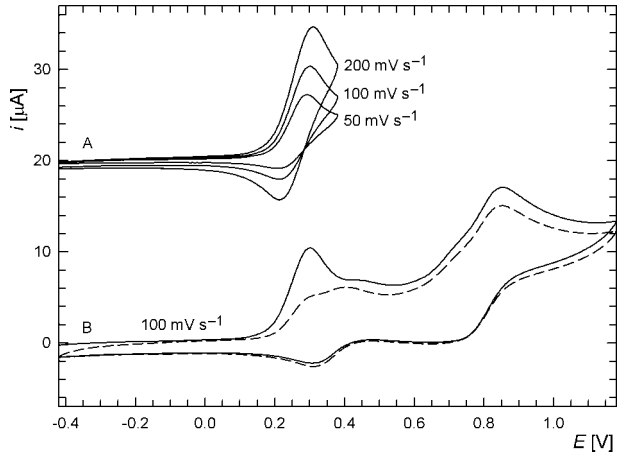

Figure 10. Cyclic voltammograms of **1** (in CH_2Cl_2 at Pt electrode). The partial voltammogram is started at +20 μA to avoid overlaps (for B: full line = first scan, dashed line = second scan).

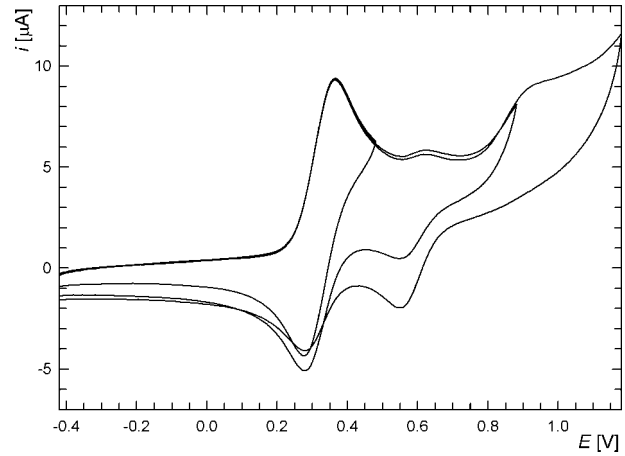

Figure 11. Cyclic voltammograms of complex **10** (in CH_2Cl_2 at a Pt electrode, scan rate 100 mV s^{-1}).

and 0.19 for PPh_2). When the switching potential is increased, an additional follow-up peak emerges. The second oxidative peak develops more at slower scan rates and after increasing the switching potential. Upon back scanning, its corresponding cathodic counter-peak is detected (E_{pa}/E_{pc} = 0.40/0.31 V). Depending on the scan rate, the new wave convolutes with or almost entirely replaces wave I (Figure 10, B). Finally, when the scan range is extended even further, additional irreversible oxidation is observed at E_{pa} = 0.86 V (wave II), attributable to one-electron oxidation of the carboxamide moiety.[36] It appears likely that the initial oxidation at the ferrocene unit is followed by chemical reactions giving rise to another redox-active species (EC mechanism). Such behavior resulting from instability of primary electrogenerated species is not uncommon among ferrocene phosphines.[3,37]

The electrochemical behavior of **5** and **6** is similar to that of **1**. Thus, acid **5** undergoes one-electron oxidation at the ferrocene unit (E_{pa} 0.30 V, wave I), which is associated with chemical complications that make it quasi-reversible. The following oxidation of the amide moiety (wave II) is irreversible. Diamide **6** is also oxidized first in a quasi-reversible step at E_{pa} 0.29 V (wave I), but the subsequent oxidation is observed as a broad (probably composite due to oxidation of two amide groups) wave at E_{pa} ca. 0.77 V and has a counter-peak at E_{pc} 0.63 V (wave II). Phosphine oxide **3** and sulfide **4**, lacking a reactive site (lone electron pair), undergo a reversible one-electron removal[38] at 0.43 V. Anodic shift of this ferrocene/ferrocenium wave corresponds with an increased electron-withdrawing character of the substituents (σ_P:[35] 0.53 for $P(O)Ph_2$ and 0.47 for $P(S)Ph_2$).

Redox behavior of complexes **10** (Figure 11) and **12** parallels that of **1** only partly. Both compounds undergo an essentially *reversible* ferrocene oxidation (wave I) at 0.32 V (ΔE_p = 80 mV) for **10** and at 0.21 V (ΔE_p = 85 mV) for **12**. In the case of **10**, the observed anodic shift of wave I (vs **1**) is in line with electron density transfer upon coordination (ligand → Pd), which renders any electron removal from the ferrocene unit more difficult. The opposite shift observed for **12** likely reflects the anionic nature of the ferrocene ligand. When the CV scans on **10** and **12** are performed further beyond the first wave (i.e., toward more positive potentials), the voltammograms change. For **10**, an additional minor redox couple develops ($E^{\circ\prime}$ = 0.59 V) on account of the first wave ($i_{pa}(I) \approx i_{pc}(I) + i_{pc}$(new wave)) and becomes better resolved during the second scan and after scanning to higher potentials. Upon increasing the switching potential even further, a minor irreversible oxidation emerges (wave II; $E_{pa} \approx$ 0.93 V). For **12**, these additional oxidative peaks are hardly discernible (no free CONH group is present in **12**), while two cathodic peaks at E_{pa} ca. +0.52 and +0.22 V can be detected during back scanning, the latter convoluting with the reduction counter-wave due to first oxidation (wave I). In contrast, the redox response of complex **11** is rather simple, the compound showing a single reversible wave attributable to ferrocene oxidation. The pronounced anodic shift of the ferrocene/ferrocenium wave (by 330 mV vs **1**) can be accounted for a synergy between **1**-to-Pd donation and positive charge of the complex species.

Catalytic Tests. Because of their polar nature, the phosphinoferrocene Gly-carboxamides could turn into potentially useful ligands for catalysis in organic solvents. Replacement of hazardous organic solvents for environmentally benign ones and for water remains a challenging task, as it not only helps in minimizing waste production and energy consumption during product isolation but may also aid catalyst recovery and recycling.[10,39] The catalytic potential of the compounds under study was assessed in palladium-catalyzed Suzuki−Miyaura cross-coupling,[40] using catalysts generated *in situ* from palladium(II) acetate and phosphines **1**, **5**, **6**, or Hdpf (1.2 equiv vs Pd), and the model coupling of phenylboronic acid to 4-bro-

(33) The compounds do not undergo defined reductions (ill-defined or none at all) in the potential window provided by the solvent and, therefore, were studied mainly in the anodic region.

(34) Definitions: E_{pa} and i_{pa} are anodic peak potential and anodic peak current, respectively. Parameters of cathodic processes are denoted similarly (E_{pc} and i_{pc}). Separation of the peaks: $\Delta E_p = E_{pa} - E_{pc}$.

(35) Hansch, C.; Leo, A.; Taft, R. W. *Chem. Rev.* **1991**, *91*, 165.

(36) Weinberg, N. L.; Weinberg, H. R. *Chem. Rev.* **1968**, *68*, 449.

(37) (a) Ong, J. H. L.; Nataro, C.; Golen, J. A.; Rheingold, A. L. *Organometallics* **2003**, *22*, 5027. (b) Zanello, P.; Opromolla, G.; Giorgi, G.; Sasso, G.; Togni, A. *J. Organomet. Chem.* **1996**, *506*, 61. (c) Pilloni, G.; Longato, B.; Corain, B. *J. Organomet. Chem.* **1991**, *420*, 57.

(38) An additional oxidative peak is observed for **4** ($E_{pa} \approx$ 1.0 V), probably due to amide oxidation.

(39) (a) Shaughnessy, K. H. *Eur. J. Org. Chem.* **2006**, 1827. (b) Li, C.-J. *Chem. Rev.* **2005**, *105*, 3095. (c) Franzén, R.; Xu, Y. *Can. J. Chem.* **2005**, *83*, 266. (d) Pinault, N.; Bruce, D. W. *Coord. Chem. Rev.* **2003**, *241*, 1.

(40) (a) Miyaura, N. *Metal-Catalyzed Cross-Coupling Reactions of Organoboron Compounds with Organic Halides in Metal-Catalyzed Cross-Coupling Reactions*, 2nd ed.; de Meijere, A. ; Diederich, F., Eds.; Wiley-VCH: Weinheim 2004; Vol. 1, Chapter 2, pp 41−123. (b) Miayura, N.; Suzuki, A. *Chem. Rev.* **1995**, *95*, 2457. (c) Suzuki, A. *J. Organomet. Chem.* **1999**, *576*, 147. (d) Miyaura, N. *Top. Curr. Chem.* **2002**, *219*, 11.

Scheme 4. Suzuki−Miyaura Cross-Coupling of 4-Bromotoluene to Give Biphenyl 13

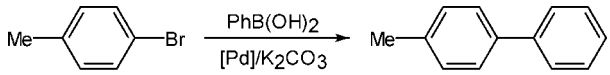

13

Table 6. Catalytic Results Obtained with the 5/Pd(OAc)$_2$ System in Different Solvents[a]

		yield of **13** (%)[b]	
entry	solvent	t = 6 h	t = 16 h
1	dioxane	95 (89)	100 (97)
2	dioxane/H_2O	100 (96)	100 (98)
3	EtOH	100 (92)	100 (93)
4	EtOH/H_2O	100 (94)	100 (95)
5	H_2O	95 (91)	100 (93)
6	toluene/H_2O	50 (−)	49 (−)

[a] 4-Bromotoluene (1.0 mmol), phenylboronic acid (1.2 mmol), K_2CO_3 (2 mmol) in the appropriate solvent (5 mL). Reactions were performed with 0.5 mol % Pd catalyst at 80 °C for 6 or 16 h. [b] NMR yield (isolated yield in parentheses). The results are an average of two independent runs.

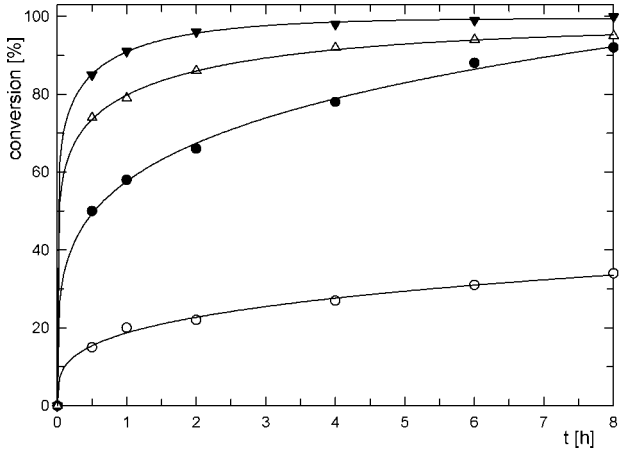

Figure 12. Kinetic profiles for the coupling reactions performed in dioxane and in dioxane/water (1:1): Pd(OAc)$_2$/**5** in dioxane (●), Pd(OAc)$_2$/**5** in dioxane/water (▼), Pd(OAc)$_2$ in dioxane (○), Pd(OAc)$_2$ in dioxane/water (Δ). Conditions: 0.5 mol % Pd catalyst, 80 °C.

motoluene (a deactivated substrate) to give 4-methylbiphenyl (**13**; Scheme 4).

Initial tests were carried out in ethanol and dioxane, in their aqueous mixtures (1:1 v/v), and also in pure water, all at 80 °C and in the presence of 0.5 mol % palladium catalyst based on acid **5** as the most polar donor in the series. The results (Table 6) already indicated that the coupling reaction proceeds rapidly and with excellent conversions in all homogeneous reaction media. In contrast, the results obtained in a toluene/water biphasic mixture were rather disappointing, as the conversion reached only ca. 50% within 6 h and did not increase any further.

Subsequent kinetic experiments in dioxane and in dioxane/water revealed (i) that the **5**/Pd(OAc)$_2$ catalytic system is much more efficient than the corresponding ligand-free catalysts (i.e., Pd(OAc)$_2$ itself) and (ii) that the reaction proceeds faster in a dioxane/water mixture than in dioxane itself (Figure 12). A considerably higher activity of the phosphine-supported catalyst was noted also in water (Figure 13). Apparently, the polar phosphine stabilizes the catalytically active species (via P-coordination) and positively affects its solubility (stability) in polar reaction media, acting as a surfactant-like anionic carboxylate. The beneficiary effect of the polar side chain in **5** was corroborated through a comparison of the results obtained with Pd(OAc)$_2$/L (L = **1**, **5**, and **6**) and Pd(OAc)$_2$/Hdpf catalysts at shorter reaction times (i.e., at lower conversions; Table 7). In all solvents tested, the reaction with the former system involving Hdpf Gly-amides possessing extended polar pendants gave better yields that the Hdpf-based catalyst. Furthermore, the catalyst supported with acid **5** showed the least pronounced dependence of its catalytic performance on the nature of the reaction solvent and exerted practically the same or better activity than other Gly-Hdpf amides (Table 7).

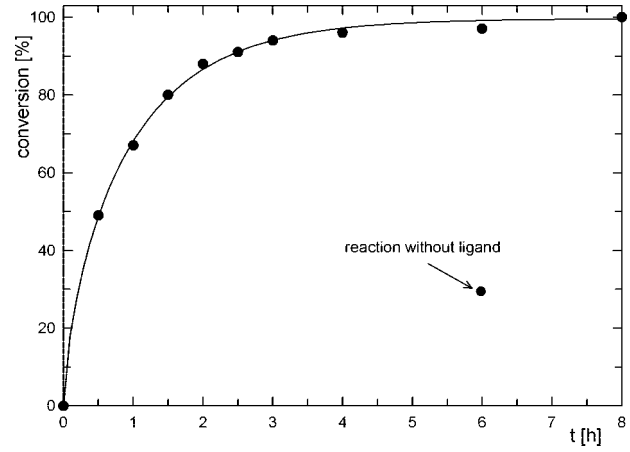

Figure 13. Kinetic profile of the coupling reaction performed in water with Pd(OAc)$_2$/**5** catalyst. The conversion attained with a ligandless catalyst after 6 h is indicated for comparison. Conditions: 0.5 mol % Pd catalyst, 80 °C.

Table 7. Comparison of Catalytic Efficiency of Phosphinoamide- and Hdpf-Supported Catalysts in Various Solvents[a]

		yield of **13** (%)[b]			
entry	solvent	[Pd]/**1**	[Pd]/**5**	[Pd]/**6**	[Pd]/Hdpf
1	dioxane	57	66	55	22
2	dioxane/H_2O	100	96	99	86
3	EtOH	96	98	94	94
4	EtOH/H_2O	98	97	100	51
5	H_2O	81	88	71	75

[a] 4-Bromotoluene (1.0 mmol), phenylboronic acid (1.2 mmol), K_2CO_3 (2 mmol) in the appropriate solvent (5 mL). Reactions were performed with 0.5 mol % Pd catalyst at 80 °C for only 2 h ([Pd] = Pd(OAc)$_2$). [b] The yields were determined from integration of ^{1}H NMR spectra.

Since the best catalytic results were obtained in ethanol and in ethanol/water (1:1), these solvents were studied in more detail and compared with pure water (Table 8). Coupling reactions in ethanolic media proceeded significantly faster than in other solvents tested but with only a marginal effect of the supporting ligand. The efficiency of Pd(OAc)$_2$ and **5**/Pd(OAc)$_2$ catalysts was practically equal, the former system exerting somewhat lower conversions in ethanol and higher conversions in ethanol/water. This acceleration can be attributed to a mild reducing ability of ethanol facilitating the generation of a molecular catalyst (L_nPd^0) or catalytically active, solvent- and ligand-stabilized fine metal particles.[41] Upon decreasing the catalyst amount to 0.1 and 0.05 mol %, the reactions still proceeded with good to excellent yields *within 30 min*, particularly in aqueous ethanol, where the turnover frequencies (TOFs) exceeded 3600 mmol product (mmol Pd)$^{-1}$ h^{-1}. At 0.01 mol % catalyst loading, the conversions dropped below 50% even in

(41) Astruc, D. *Inorg. Chem.* **2007**, *46*, 1884, and references therein.

Table 8. Comparison of Catalytic Results Obtained in Ethanol, Aqueous Ethanol, and Water[a]

	yield to **13** (%)					
reaction time (h)	[Pd]/**5** in EtOH	[Pd] in in EtOH	[Pd]/**5** in EtOH/H_2O	[Pd] in EtOH/H_2O	[Pd]/**5** in H_2O	[Pd] in H_2O
0.5	95	90	95	100	49	4
1.0	98	92	96	100	67[e]	8
2.0	98	93	97	100	88	16
4.0	98	93	98	100	96	n.a.
6.0	99	93	98	100	97	30
0.5[b]	91	70	94	95	28	5
0.5[c]	83	65	91	92	7	4
0.5[d]	21	14	49	35	n.a.	n.a.

[a] 4-Bromotoluene (1.0 mmol), phenylboronic acid (1.2 mmol), and K_2CO_3 (2 mmol) were reacted in the appropriate solvent (5 mL) in the presence of 0.5 mol % Pd catalyst at 80 °C for the reaction time specified. [Pd] = $Pd(OAc)_2$. [b] 0.1 mol % Pd catalyst. [c] 0.05 mol % Pd. [d] 0.01 mol % Pd. [e] Under identical conditions (0.5 mol % Pd, 1 h), the analogous catalysts [Pd]/**1** and [Pd]/**6** afforded 60% and 51% yields of the coupling product, respectively.

the best solvent (Table 8).[42] As opposed to ethanolic media, the efficiency of both catalytic systems differed dramatically in pure water (Table 8). Only the phosphine-supported catalyst gave good conversions, with acid **5** performing better than compounds **1** and **6**.

Concluding Remarks. Amide coupling of Hdpf with glycine esters smoothly affords novel organometallic phosphino-carboxamides. These donors can be designed in modular fashion, allowing for facile modifications at both the ferrocene moiety (e.g., through variation of the phosphorus groups) and in the amino acid moiety (e.g., by modification at the carboxyl group or by changing the amino acid moiety). The multidonor nature of these ligands results in their high coordination versatility, already demonstrated by the series of (L^{NC})Pd complexes prepared form the archetypal ligand **1**. When the amino acid pendant groups remain uncoordinated, they can be utilized for the construction of defined supramolecular networks (see the structures of **9** and **9a**, in which the molecular arrays propagate via a combination of dative and hydrogen bonds, *differently* for both solvatomorphs). Alternatively, a free amino acid pendant increases the solubility of these donors in polar organic solvents and in water, making the phosphinoferrocene carboxamides attractive as ligands for catalysis in such "greener" reaction media.

Experimental Section

Materials and Methods. Unless noted otherwise, the syntheses were performed under an argon atmosphere and with exclusion of direct daylight. Hdpf,[3] glycine methyl ester hydrochloride,[43] [$PdCl_2$(cod)],[44] and di-μ-chloridobis{[(2-dimethylamino-κN)methyl]phenyl-κC^1}dipalladium(II)[45] were prepared by the literature procedures. Solvents used in the syntheses were dried by standing over appropriate drying agents and distilled under argon: dichloromethane and chloroform (K_2CO_3), dioxane (sodium), acetonitrile (P_2O_5). Methanol was distilled from MeONa. Other chemicals (Fluka, Aldrich) and solvents used for crystallizations and in chromatography were used without further purification.

NMR spectra were measured with a Varian Unity Inova spectrometer (^{1}H, 399.95; ^{13}C, 100.58; ^{31}P, 161.90 MHz) at 25 °C. Chemical shifts (δ) are given relative to internal $SiMe_4$ (^{13}C and ^{1}H) or to external 85% aqueous H_3PO_4 (^{31}P). In addition to the standard notation of the signal multiplicity, vt and vq are used to distinguish virtual triplets and quartets ($J' = 1.8-2.0$ Hz) arising from magnetically nonequivalent protons in the AA′BB′ and AA′BB′X spin systems (X = ^{31}P) of the ferrocene unit. IR spectra were recorded with an FT IR Nicolet Magna 650 spectrometer in the range 400−4000 cm^{-1}. Positive ion electron impact (EI) and fast atom bombardment (FAB) mass spectra were obtained on a VG Analytical ZAB EQ spectrometer. Electrospray (ESI) mass spectra were recorded with a Bruker Esquire 3000 or with a Thermo Scientific LTQ Orbitrap XL spectrometers. Samples were dissolved in a little dichloromethane or dimethylsulfoxide and then diluted with methanol. Melting points were determined on a Kofler block.

Electrochemical measurements were carried out with a computer-controlled μAUTOLAB III (Eco Chemie) multipurpose potentiostat at room temperature using a standard three-electrode cell equipped with a platinum disk (AUTOLAB RDE, 3 mm diameter) as the working electrode, platinum sheet auxiliary electrode, and saturated calomel reference electrode (SCE) separated by a salt bridge. Samples were dissolved in dichloromethane (Fluka, absolute, declared H_2O content below 0.005%) to give a solution containing ca. 5×10^{-4} M of the analyte and 0.1 M $Bu_4N[PF_6]$ (Fluka, purissimum for electrochemistry). The solutions were deaerated with argon before the measurement and then kept under an argon blanket. The potentials are given relative to a ferrocene/ferrocenium reference.

Safety Note. Caution! Although we have not encountered any problems, it should be noted that perchlorate salts of metal complexes with organic ligands are potentially explosive and should be handled only in small quantities and with care.

Preparation of 1-(Diphenylphosphino)-1′-{*N*-[(methoxycarbonyl)methyl]carbamoyl}ferrocene (1). Hdpf (4.15 g, 10 mmol) and 1-hydroxybenzotriazole (1.62 g, 12 mmol) were dissolved in dichloromethane (90 mL). The solution was cooled in an ice bath and treated with *N*-(3-dimethylaminopropyl)-*N*′-ethylcarbodiimide (2.10 mL, 12 mmol). After stirring at 0 °C for 30 min, a mixture of [$H_3NCH_2CO_2Me$]Cl (1.80 g, 14 mmol), triethylamine (2.25 mL, 16 mmol), and dichloromethane (90 mL) was introduced, and the cooling bath was removed. The reaction mixture was stirred overnight at room temperature and then washed with 10% aqueous citric acid (50 mL), saturated aqueous $NaHCO_3$ (2× 50 mL), and brine (50 mL). After drying over $MgSO_4$, the volatiles were removed under vacuum, and the residue was purified by flash chromatography (silica gel, dichloromethane/methanol, 10:1, v/v). A single orange band was collected and evaporated to afford analytically pure **1** as an orange solid. Yield: 4.95 g (98%).

Mp: 131−133 °C ($CHCl_3$). ^{1}H NMR ($CDCl_3$): δ 3.75 (s, 3 H, OMe), 4.07 (d, $^3J_{HH}$ = 5.6 Hz, 2 H, NHCH_2), 4.20 (vq, 2 H, fc), 4.25 (vt, 2 H, fc), 4.50 (vt, 2 H, fc), 4.60 (vt, 2 H, fc), 6.08 (t, $^3J_{HH}$ = 5.6 Hz, 1 H, NH), 7.29−7.41 (m, 10 H, PPh_2). ^{13}C{^{1}H} NMR ($CDCl_3$): δ 41.19 ($NHCH_2$), 52.30 (OMe), 69.46 (2 C, CH fc), 71.77 (2 C, CH fc), 72.96 (d, J_{PC} = 4 Hz, 2 C, CH fc), 74.43 (d, J_{PC} = 15 Hz, 2 C, CH fc), 75.75 (*C*-CONH fc), 128.26 (d, $^3J_{PC}$ = 7 Hz, 4 C, CH_m PPh_2), 128.70 (2 C, CH_p PPh_2), 133.50 (d, $^2J_{PC}$ = 19 Hz, 4 C, CH_o PPh_2), 138.49 (d, $^1J_{PC}$ = 9 Hz, 2 C, C_{ipso} PPh_2), 170.25

(42) When the less reactive 4-chlorotoluene was used instead of 4-bromotoluene as the substrate, the coupling reaction did not proceed (aqueous ethanol, 80 °C, 0.5 mol % $Pd(OAc)_2$/**5**, 24 h).

(43) (a) Meyers, A. I.; Williams, D. R.; Erickson, G. W.; White, S.; Druelinger, M. *J. Am. Chem. Soc.* **1981**, *103*, 3081. (b) Brenner, M.; Huber, W. *Helv. Chim. Acta* **1953**, *36*, 1109.

(44) Drew, D.; Doyle, J. R. *Inorg. Synth.* **1972**, *13*, 47.

(45) Cope, A. C.; Friedrich, E. C. *J. Am. Chem. Soc.* **1968**, *90*, 909.

Table 9. Crystallographic Data, Data Collection, and Structure Refinement Parameters[a]

	2	**3**	**4**	**6**	**9**	**9a**	**10**	**11**	**12**
formula	$C_{29}H_{30}FeNO_3P$	$C_{26}H_{24}FeNO_4P$	$C_{26}H_{24}FeNO_3PS$	$C_{25}H_{23}FeN_2O_2P$	$C_{58}H_{62}Cl_2Fe_2N_4O_{12}P_2Pd$[f]	$C_{54}H_{50}Cl_{14}Fe_2N_4O_4P_2Pd$[g]	$C_{35}H_{36}ClFeN_2O_3PPd$	$C_{35}H_{36}ClFeN_2O_7PPd$	$C_{35}H_{35}FeN_2O_3PPd$
M (g mol^{-1})	527.36	501.28	517.34	470.27	1358.06	1595.32	761.33	825.33	724.87
cryst syst	monoclinic	monoclinic	monoclinic	monoclinic	triclinic	triclinic	orthorhombic	monoclinic	triclinic
space group	$P2_1/c$ (no. 14)	$P2_1/c$ (no. 14)	$P2_1/c$ (no. 14)	$P2_1/c$ (no. 14)	$P\bar{1}$ (no. 2)	$P\bar{1}$ (no. 2)	$Pca2_1$ (no. 29)	$P2_1/c$ (no. 14)	$P\bar{1}$ (no. 2)
a (Å)	11.7617(2)	15.633(3)	8.7237(1)	15.6965(2)	9.4105(4)	9.2009(3)	17.1588(1)	10.6325(1)	12.0143(2)
b (Å)	23.4217(5)	11.060(2)	14.2178(2)	7.6869(1)	9.7835(3)	12.6363(4)	14.1784(2)	19.8750(2)	15.4376(2)
c (Å)	9.9834(2)	13.060(2)	19.2276(3)	17.9425(3)	17.7049(8)	14.8709(4)	26.8028(3)	16.2634(2)	16.8762(2)
α (deg)					103.067(3)	104.651(2)			91.9417(9)
β (deg)	111.0971(9)	94.67(2)	91.3849(9)	93.4216(9)	93.042(2)	105.531(2)		103.7658(7)	97.083(1)
γ (deg)					111.947(2)	92.374(2)			100.1766(9)
V (Å^3)	2565.87(9)	2250.6(7)	2384.14(6)	2161.04(5)	1455.6(1)	1600.59(8)	6520.7(1)	3338.08(6)	3052.34(7)
Z	4	4	4	4	1	1	8	4	4
D_{calc} (g mL^{-1})	1.365	1.479	1.441	1.445	1.549	1.655	1.551	1.642	1.577
μ(Mo Kα) (mm^{-1})	0.681	0.776	0.816	0.797	1.009	1.407[h]	1.165[j]	1.154[k]	1.156[h]
$2\theta_{max}$ (deg)	27.5	26.6	27.5	27.5	27.5	27.5	26.2	27.5	27.5
diffrns total	37 020	29 226	40 378	43 599	26 875	30 275	92 014	56 512	55 435
R_{int} (%)[b]	1.33	5.04	1.16	1.71	4.31	2.89	5.09	3.84	2.02
unique/obsd[c] diffrns	5869/5270	4719/3986	5472/4894	4955/4147	6660/4649	7351/5753	12 863/11209	7629/6823	14 007/11 727
R (obsd data) (%)[c,d]	2.76	2.81	2.60	4.37	4.13	5.09	3.06	2.85	2.87
R, wR (all data) (%)[c,d]	3.28, 6.77	3.39, 8.28	3.12, 6.56	5.49, 12.3	7.84, 8.78	7.11, 13.2	4.12, 6.88	3.38, 7.03	3.98, 6.99
$\Delta\rho$ (e Å^{-3})	0.32, −0.46	0.39, −0.40	0.29, −0.29	2.14,[e] −0.59	0.47, −0.63	1.39, −1.27[j]	0.51, −0.65	0.80, −0.81	0.73, −0.76
CCDC entry	723117	723118	723119	723120	723121	723122	723123	723124	723125

[a] Common details: T = 150(2) K. [b] $R_{int} = \sum|F_o^2 - F_o^2(\text{mean})|/\sum F_o^2$, where $F_o^2(\text{mean})$ is the average intensity for symmetry-equivalent diffractions. [c] Diffractions with $I_o > 2\sigma(I_o)$. [d] $R = \sum||F_o| - |F_c||/\sum|F_o|$, $wR = [\sum\{w(F_o^2 - F_c^2)^2\}/\sum w(F_o^2)^2]^{1/2}$. [e] See Experimental Part for the explanation of the high residual electron density. [f] $C_{50}H_{46}Cl_2Fe_2N_4O_4P_2Pd \cdot 4C_2H_4O_2$. [g] $C_{50}H_{46}Cl_2Fe_2N_4O_4P_2Pd \cdot 4CHCl_3$. [h] Absorption was neglected due to crystal shape or defects. [i] Residual electron density in the space accommodating partly disordered solvent molecules. [j] Corrected for absorption. TF = 0.740−0.907. [k] Corrected for absorption. TF = 0.666−0.919.

(CONH), 170.51 (CO_2Me); the signal due *C*-P of fc is obscured by the solvent resonance. $^{31}P\{^1H\}$ NMR ($CDCl_3$): δ −16.9 (s). IR (Nujol): ν/cm^{-1} ν_{NH} 3332 s, ν_{CO}(ester) 1758 vs, amide I 1650 vs, amide II 1544 vs, 1439 s, 1403 m, 1360 m, 1313 m, 1208 s, 1182 s, 1029 m, 836 w, 825 w, 747 m, 697 s, 489 m. MS (EI+): *m*/*z* (relative abundance) 485 (100, $M^{+\cdot}$), 454 (5, $[M - OMe]^+$), 412 (80, $[M - CH_2CO_2Me]^+$), 397 (8), 370 (6), 321 (55, "$[Fe(C_5H_4PPh_2)O]^+$"), 305 (15), 266 (20), 226 (16), 201 (56, $[Ph_2PO]^+$), 183 (18, $[PPh_2 - 2H]^+$), 171 (24), 149 (45), 121 (15, $[FeC_5H_5]^+$), 115 (23), 98 (17), 83 (31), 55 (59). HR-MS (EI+): calcd for $C_{26}H_{24}NO_3P^{56}Fe$ ($M^{+\bullet}$) 485.0843, found 485.0821. Anal. Calcd for $C_{26}H_{24}NO_3PFe$: C 64.35, H 4.99, N 2.89. Found: C 64.29, H 4.89, N 2.85.

Preparation of 1-(Diphenylphosphino)-1′-{*N*-[(*tert*-butyloxycarbonyl)methyl]carbamoyl}ferrocene (2). Compound **2** was prepared similarly to **1**, starting with Hdpf (414 mg, 1.0 mmol), 1-hydroxybenzotriazole (162 mg, 1.2 mmol), *N*-(3-dimethylaminopropyl)-*N*′-ethylcarbodiimide (186 mg, 1.2 mmol), $[H_3NCH_2CO_2CMe_3]Cl$ (201 mg, 1.2 mmol), and triethylamine (0.17 mL, 1.2 mmol). Isolation as above afforded **2** as an orange solid. Yield: 501 mg (95%).

Mp: 130−132 °C ($CHCl_3$). ^1H NMR ($CDCl_3$): δ 1.49 (s, 9 H, C*Me*$_3$), 3.97 (d, $^3J_{HH}$ = 5.2 Hz, 2 H, NHC*H*$_2$), 4.19 (vq, 2 H, fc), 4.24 (vt, 2 H, fc), 4.48 (vt, 2 H, fc), 4.59 (vt, 2 H, fc), 6.05 (t, $^3J_{HH}$ = 5.2 Hz, 1 H, NH), 7.29−7.40 (m, 10 H, PPh_2). $^{13}C\{^1H\}$ NMR ($CDCl_3$): δ 28.10 (3 C, C*Me*$_3$), 41.99 ($NHCH_2$), 69.38 (2 C, CH fc), 71.79 (d, $J \approx 1$ Hz, 2 C, CH fc), 73.10 (d, J_{PC} = 4 Hz, 2 C, CH fc), 74.40 (d, J_{PC} = 14 Hz, 2 C, CH fc), 76.21 (*C*-CONH fc), 82.05 (*C*Me$_3$), 128.28 (d, $^3J_{PC}$ = 7 Hz, 4 C, CH_m PPh_2), 128.78 (2 C, CH_p PPh_2), 133.50 (d, $^2J_{PC}$ = 19 Hz, 4 C, CH_o PPh_2), 138.17 (d, $^1J_{PC}$ = 7 Hz, 2 C, C_{ipso} PPh_2), 169.22, 169.93 (2× C═O); the signal due to *C*(fc)-P is obscured by the solvent resonance. $^{31}P\{^1H\}$ NMR ($CDCl_3$): δ −16.9 (s). IR (Nujol): ν/cm^{-1} ν_{NH} 3296 w, ν_{CO} (ester) 1743 vs, amide I 1640 vs, amide II 1539 vs, 1305 m, 1224 s, 1154 vs, 1093 w, 1069 w, 1028 m, 999 w, 905 w, 889 w, 844 m, 771 w, 744 s, 697 s, 496 m. MS (EI+): *m*/*z* (relative abundance) 528 (35, $M^{+\cdot}$), 454 (5, $[M - OCMe_3]^+$), 427 (10), 412 (45, $[M - CH_2CO_2CMe_3]^+$), 397 (7), 370 (6), 320 (25, "$[Fe(C_5H_4PPh_2)O]^+$"), 304 (10), 225 (9), 200 (20, $[Ph_2PO]^+$), 183 (11, $[Ph_2P - 2H]^+$), 170 (15), 149 (9), 136 (10), 120 (9, $[FeC_5H_5]^+$), 114 (7), 94 (15), 81 (38), 55 (71). HR-MS (EI+): calcd for $C_{29}H_{30}NO_3P^{56}Fe$ ($M^{+\cdot}$) 527.1313, found 527.1329. Anal. Calcd for $C_{29}H_{30}NO_3PFe$: C 66.04, H 5.73, N 2.66. Found: C 65.88, H 5.53, N 2.77.

Preparation of 1-(Diphenylphosphinoyl)-1′-{*N*-[(methoxycarbonyl)methyl]carbamoyl}ferrocene (3). In air, hydrogen peroxide (0.10 mL 30%, 0.8 mmol) was added dropwise to an ice-cooled solution of **1** (123 mg, 0.25 mmol) in acetone (10 mL). The mixture was stirred at 0 °C for 30 min and diluted with water (5 mL) and 10% aqueous $Na_2S_2O_3$ (1 mL). The acetone was removed under reduced pressure, and the aqueous residue was extracted with chloroform (2× 10 mL). Combined organic extracts were washed with brine, dried ($MgSO_4$), and evaporated. The solid residue was dissolved in ethyl acetate (3 mL), and the solution filtered (PTFE syringe filter, pore size 0.45 μmm) and carefully layered with hexane (8 mL). Crystallization by liquid-phase diffusion over several days afforded **3** as orange crystals, which were isolated by suction and dried in air. Yield: 122 mg (96%).

Mp: 201−203 °C (ethyl acetate). ^1H NMR ($CDCl_3$): δ 3.62 (s, 3 H, OMe), 4.12 (d, $^3J_{HH}$ = 6.1 Hz, 2 H, NHC*H*$_2$), 4.12 (vt, 2 H, fc), 4.51 (vq, 2 H, fc), 4.61 (vq, 2 H, fc), 5.06 (vt, 2 H, fc), 7.44−7.73 (m, 10 H, PPh_2), 9.49 (t, $^3J_{HH}$ = 6.1 Hz, 1 H, NH). $^{13}C\{^1H\}$ NMR ($CDCl_3$): δ 41.36 ($NHCH_2$), 51.84 (OMe), 70.54 (2 C, CH fc), 70.87 (2 C, CH fc), 72.76 (d, J_{PC} = 10 Hz, 2 C, CH fc), 73.28 (d, $^1J_{PC}$ = 115 Hz, *C*-P fc), 75.21 (d, J_{PC} = 13 Hz, 2 C, CH fc), 78.26 (*C*-CONH fc), 128.43 (d, $^3J_{PC}$ = 12 Hz, 4 C, CH_m PPh_2), 131.48 (d, $^2J_{PC}$ = 10 Hz, 4 C, CH_o PPh_2), 131.93 (d, $^4J_{PC}$ = 3 Hz, 2 C, CH_p PPh_2), 132.87 (d, $^1J_{PC}$ = 108 Hz, 2 C, C_{ipso} PPh_2), 170.72, 170.80 (2 × C═O). $^{31}P\{^1H\}$ NMR ($CDCl_3$): δ 32.1 (s). IR (Nujol):

ν/cm^{-1} ν_{NH} 3223 w, ν_{CO}(ester) 1754 vs, amide I 1664 vs, amide II 1551 s, 1306 s, 1209 m, 1197 s, 1155 vs, 1119 s, 1068 w, 1047 w, 1036 w, 1001 w, 978 w, 854 w, 844 w, 823 w, 753 m, 703 s, 571 s, 537 s, 531 m, 515 m, 498 m, 483 w. MS (EI+): *m/z* (relative abundance) 501 (36, $M^{+\bullet}$), 470 (2, $[M - OMe]^+$), 413 (2, $[M - NHCH_2CO_2Me]^+$), 386 (2), 338 (2), 321 (15, "$[Fe(C_5H_4PPh_2)O]^{+\bullet}$"), 256 (5), 201 (4, $[Ph_2PO]^+$), 149 (10), 137 (10), 109 (11), 97 (20), 85 (49), 83 (77), 69 (100), 55 (63). HR-MS (EI+): calcd for $C_{26}H_{24}NO_4P^{56}Fe$ ($M^{+\bullet}$) 501.0792, found 501.0782. Anal. Calcd for $C_{26}H_{24}NO_4PFe$: C 62.29, H 4.83, N 2.79. Found: C 62.28, H 4.83, N 2.66.

Preparation of 1-(Diphenylthiophosphoryl)-1′-{*N*-[(methoxycarbonyl)methyl]carbamoyl}ferrocene (4). A solution of **1** (128 mg, 0.26 mmol) and sulfur (12 mg, 0.37 mmol) in ethyl acetate (30 mL) was heated at reflux for 90 min. The mixture was cooled to room temperature and evaporated. Purification by flash chromatography (silica gel, dichloromethane/methanol, 20:1, v/v) followed by evaporation afforded **4** as an orange solid. Yield: 134 mg (98%).

Mp: 153−155 °C (toluene). ^{1}H NMR ($CDCl_3$): δ 3.76 (s, 3 H, OMe), 4.02 (vt, 2 H, fc), 4.10 (d, $^3J_{HH}$ = 6.1 Hz, 2 H, NHC*H*$_2$), 4.49 (vq, 2 H, fc), 4.66 (vq, 2 H, fc), 4.95 (vt, 2 H, fc), 7.42−7.76 (m, 10 H, PPh_2), 7.85 (t, $^3J_{HH}$ = 6.1 Hz, 1 H, NH). ^{13}C{^{1}H} NMR ($CDCl_3$): δ 41.11 ($NHCH_2$), 52.18 (OMe), 71.11 (2 C, CH fc), 71.26 (2 C, CH fc), 73.28 (d, J_{PC} = 10 Hz, 2 C, CH fc), 75.08 (d, J_{PC} = 13 Hz, 2 C, CH fc), 76.10 (d, $^1J_{PC}$ = 97 Hz, *C*-P fc), 77.68 (*C*-CONH fc), 128.38 (d, $^3J_{PC}$ = 13 Hz, 4 C, CH_m PPh_2), 131.60 (d, $^4J_{PC}$ = 3 Hz, 2 C, CH_p PPh_2), 131.62 (d, $^2J_{PC}$ = 10 Hz, 4 C, CH_o PPh_2), 133.45 (d, $^1J_{PC}$ = 87 Hz, 2 C, C_{ipso} PPh_2), 170.13, 170.39 (2× C═O). ^{31}P{^{1}H} NMR ($CDCl_3$): δ 42.9 (s). IR (neat, ATR): ν/cm^{-1} ν_{NH} 3295 m, ν_{CO}(ester) 1750 vs, amide I 1648 vs, amide II 1535 vs, 1305 m, 1174 s, 1102 s, 1028 s, 1001 m, 978 m, 836 m, 749 s, 713 vs, 693 s, 652 s, 538 m, 484 s. MS (EI+): *m/z* (relative abundance) 517 (100, $M^{+\bullet}$), 486 (3, $[M - OMe]^+$), 429 (3, $[M - NHCH_2CO_2Me]^+$), 386 (6), 368 (5), 337 (64, "$[Fe(C_5H_4PPh_2)S]^{+\bullet}$"), 321 (7), 273 (6), 256 (8), 217 (7, Ph_2PS^+), 183 (14), 171 (10), 129 (12), 111 (14), 97 (28), 69 (54), 55 (83). HR-MS (EI+): calcd for $C_{26}H_{24}NO_3PS^{56}Fe$ ($M^{+\bullet}$) 517.0564, found 517.0553. Anal. Calcd for $C_{26}H_{24}NO_3PSFe$: C 60.36, H 4.68, N 2.71. Found: C 60.18, H 4.63, N 2.63.

Preparation of 1-(Diphenylphosphino)-1′-[*N*-(carboxymethyl)carbamoyl]ferrocene (5). Aqueous sodium hydroxide (200 mg, 5.0 mmol in 17 mL of deoxygenated water) was added to a solution of **1** in dioxane (485 mg, 1.0 mmol in 17 mL), and the mixture was heated to 50 °C overnight. The reaction mixture was cooled in ice, acidified with 85% H_3PO_4 to pH ≈ 2, and extracted with dichloromethane. The organic layer was dried ($MgSO_4$) and evaporated, leaving a brown residue, which was purified flash chromatography (silica gel, dichloromethane/methanol, 1:1, v/v). The single orange band was collected and evaporated under vacuum, and the residue was dried over sodium hydroxide to give acid **5** as a glassy orange solid. Yield: 446 mg (95%). The product typically contains traces of the corresponding phosphine oxide, which cannot be efficiently removed by chromatography or crystallization.

^{1}H NMR (DMSO): δ 3.68 (d, $^3J_{HH}$ = 5.6 Hz, 2 H, NHC*H*$_2$), 4.11 (vq, 2 H, fc), 4.13 (vt, 2 H, fc), 4.53 (vt, 2 H, fc), 4.68 (vt, 2 H, fc), 7.80 (t, $^3J_{HH}$ = 5.6 Hz, 1 H, N*H*), 7.26−7.41 (m, 10 H, PPh_2). ^{13}C{^{1}H} NMR (DMSO): δ 41.99 ($NHCH_2$), 68.76 (2 C, CH fc), 71.20 (2 C, CH fc), 73.05 (d, J_{PC} = 4 Hz, 2 C, CH fc), 74.47 (d, J_{PC} = 15 Hz, 2 C, CH fc), 76.45 (d, $^1J_{PC}$ = 9 Hz, *C*-P fc), 77.07 (*C*-CONH fc), 128.20 (d, $^3J_{PC}$ = 7 Hz, 4 C, CH_m PPh_2), 128.52 (2 C, CH_p PPh_2), 132.90 (d, $^2J_{PC}$ = 20 Hz, 4 C, CH_o PPh_2), 138.36 (d, $^1J_{PC}$ = 10 Hz, 2 C, C_{ipso} PPh_2), 168.21, 172.19 (2× C═O). ^{31}P{^{1}H} NMR (DMSO): δ −18.0 (s). IR (Nujol): ν/cm^{-1} ν_{NH} 3335 w, ν_{CO} (carboxyl) 1732 s, amide I 1637 vs, amide II 1538 vs, 1303 m, 1193 m, 1160 m, 1119 m, 1027 m, 999 w, 888 w, 872 m, 833 m, 743 vs, 698 vs, 634 w, 613 w, 570 w, 493 s, 452 m. HR-MS (FAB+): calcd for $C_{25}H_{22}NO_3P^{56}FeK$ ($[M + K]^+$) 510.0324, found 510.0300.

Preparation of 1-(Diphenylphosphino)-1′-[*N*-(carbamoylmethyl)carbamoyl]ferrocene (6). A solution of ester **1** (49 mg, 0.10 mmol) in methanol (5 mL) was added to liquid ammonia (5 mL) while cooling to ca. −75 °C. After the addition, the cooling bath was removed and the mixture was stirred at room temperature for 5 h. The volatiles were removed under vacuum, and the residue was purified by column chromatography (silica gel, dichlormethane/methanol, 5:1, v/v). Evaporation left an orange solid, which was crystallized from ethyl acetate/hexane at 5 °C. The separated crystalline product was filtered off, washed with hexane, and dried under vacuum to afford **6** as an orange solid. Yield: 35 mg (88%).

^{1}H NMR ($CDCl_3$): δ 4.00 (d, $^3J_{HH}$ = 5.5 Hz, 2 H, NHC*H*$_2$), 4.14 (vq, 2 H, fc), 4.25 (vt, 2 H, fc), 4.45 (vt, 2 H, fc), 4.63 (vt, 2 H, fc), 5.64 br s, 1 H, CON*H*$_2$), 6.53 (br s, 1 H, CON*H*$_2$), 6.54 (t, $^3J_{HH}$ = 5.5 Hz, 1 H, NH), 7.29−7.40 (m, 10 H, PPh_2). ^{13}C{^{1}H} NMR ($CDCl_3$): δ 43.25 ($NHCH_2$), 69.47 (2 C, CH fc), 71.98 (2 C, CH fc), 72.86 (d, J_{PC} = 3 Hz, 2 C, CH fc), 74.35 (d, J_{PC} = 15 Hz, 2 C, CH fc), 75.59 (*C*-CONH fc), 77.67 (d, J = 7 Hz, *C*-P fc), 128.29 (d, $^3J_{PC}$ = 7 Hz, 4 C, CH_m PPh_2), 128.77 (2 C, CH_p PPh_2), 133.47 (d, $^2J_{PC}$ = 20 Hz, 4 C, CH_o PPh_2), 138.35 (d, $^1J_{PC}$ = 9 Hz, 2 C, C_{ipso} PPh_2), 170.90, 171.68 (2× C═O). ^{31}P{^{1}H} NMR ($CDCl_3$): δ −17.2 (s). IR (Nujol): ν/cm^{-1} ν_{NH} 3262 m, ν_{NH} 3138 m, amide I 1694 s, amide I 1644 vs, amide II 1551 s, 1307 s, 1251 m, 1191 w, 1160 w, 1120 w, 1023 w, 996 w, 840 w, 810 w, 743 s, 699 s, 573 w, 501 m. HR-MS (ESI+): calcd for $C_{25}H_{24}{}^{56}FeN_2O_2P$ ($[M + H]^+$) 471.0925, found 471.0919. Anal. Calcd for $C_{25}H_{23}N_2O_2PFe$: C 63.85, H 4.93, N 5.96. Found: C 63.44, H 4.93, N 5.81.

Preparation of Complex 7. A solution of **1** (195 mg, 0.40 mmol) in chloroform (6 mL) was added to solid [$PdCl_2$(cod)] (52 mg, 0.20 mmol). The formed dark red solution was stirred for 1 h and then precipitated with pentane (60 mL). The separated solid was collected by filtration and dried under vacuum to give **7**. Yield: 220 mg (96%), orange solid.

^{1}H NMR ($CDCl_3$): δ 3.73 (s, 3 H, OMe), 3.93 (d, $^3J_{HH}$ = 5.7 Hz, 2 H, NHC*H*$_2$), 4.58 (vt, 2 H, fc), 4.63 (m, 2 H, fc), 4.65 (vt, 2 H, fc), 4.90 (vt, 2 H, fc), 6.52 (t, $^3J_{HH}$ = 5.7 Hz, 1 H, NH), 7.30−7.67 (m, 10 H, PPh_2). ^{13}C{^{1}H} NMR ($CDCl_3$): δ 41.10 ($NHCH_2$), 52.23 (OMe), 70.14 (2 C, CH fc), 72.98 (apparent t, J' = 27 Hz, *C*-P fc), 73.43 (2 C, CH fc), 74.05 (apparent t, J' = 4 Hz, 2 C, CH fc), 76.91 (*C*-CONH fc), ca. 77.03 (apparent t, J' = 5 Hz, 2 C, CH fc), 127.92 (apparent t, J' = 5 Hz, 4 C, CH PPh_2), 130.55 (2 C, CH PPh_2), 130.80 (apparent t, J' = 25 Hz, 2 C, C_{ipso} PPh_2), 134.12 (apparent t, J' = 6 Hz, 4 C, CH PPh_2), 169.94, 170.38 (2× C═O). ^{31}P{^{1}H} NMR ($CDCl_3$): δ 15.9 (s). IR (Nujol): ν/cm^{-1} 3238 s, 3182 w, 3106 s, 3084 m, ν_{CO}(ester) 1750 vs, amide I 1632 vs, amide II 1557 vs, 1319 m, 1307 m, 1211 s, 1199 s, 1174 s, 1096 m, 1036 m, 1006 w, 877 w, 842 w, 773 w, 743 m, 710 m, 690 m, 628 w, 517 s, 501 s, 477 m, 455 w. MS (ESI+): *m/z* 1171 ($[M + Na]^+$). Anal. Calcd for $C_{52}H_{48}N_2O_6P_2Fe_2PdCl_2$: C 54.41, H 4.22, N 2.44. Found: C 54.55, H 4.22, N 2.25.

Preparation of Complex 8. A solution of acid **5** (20 mg, 0.04 mmol) in hot glacial acetic acid (3 mL) was added to an equivalent amount of $Na_2[PdCl_4]$ dissolved in water (6 mg, 0.02 mmol in 2 mL), yielding a dark red solution that quickly deposited a microcrystalline solid. After standing for several minutes at room temperature, the solid was filtered off, washed with aqueous acetic acid (ca. 50%), and dried under vacuum. Yield: 19 mg (81%) of [$PdCl_2$(**5**-κP)$_2$]·3H_2O (**8**), red microcrystalline solid.

IR (Nujol): ν/cm^{-1} ν_{NH} 3336 w, ν_{CO} (carboxyl) 1715 vs, amide I 1606 vs, amide II 1541 vs, 1303 w, 1233 vs, 1196 w, 1166 m, 1097 m, 1061 w, 1041 m, 1030 w, 1000 w, 938 w, 834 w, 771 w, 745 s, 696 s, 627 w, 610 m, 514 vs, 498 w, 471 s, 455 w, 436 w. MS (ESI+): *m/z* 1047 ($[M - 2Cl - H]^+$), 526 ($[\mathbf{5} + O + K]^+$), 510 ($[\mathbf{5} + K]^+$). MS (ESI−): *m/z* 612 ($[Pd(\mathbf{5})Cl - 2H]^-$), 486 ([**5**

+ O − H]$^-$). Anal. Calcd for $C_{50}H_{44}N_2O_6P_2Fe_2PdCl_2 \cdot 3H_2O$: C 51.16, H 4.29, N 2.39. Found: C 50.99, H 4.10, N 2.09.

Preparation of Complex 9. A solution of **6** (19 mg, 0.04 mmol) in dichlormethane (5 mL) was added to solid [$PdCl_2$(cod)] (6 mg, 0.02 mmol). The resulting dark red solution was stirred at room temperature for 1 h and evaporated under vacuum. The residue was dissolved in hot glacial acetic acid (5 mL), and the solution was allowed to crystallize by cooling slowly to room temperature. The separated solid was filtered off, washed with 50% aqueous acetic acid and water, and dried under vacuum. Yield: 17 mg (63%) of [$PdCl_2$(**6**-κP)$_2$]$\cdot 4CH_3CO_2H$ (**9**) as an orange crystalline solid.

^{1}H NMR ($CDCl_3$): δ 2.10 (s, 6 H, CH_3CO$_2$H), 3.97 (d, $^3J_{HH}$ = 5.7 Hz, 2 H, NHCH_2), 4.55 (m, 4 H, fc), 4.63 (br s, 2 H, fc), 5.04 (vt, 2 H, fc), 6.23 (br s, 1 H, CONH_2), 6.64 (br s, 1 H, CONH_2), 7.34 (t, $^3J_{HH}$ = 5.7 Hz, 1 H, NH), 7.35−7.65 (m, 10 H, PPh_2). ^{13}C{^{1}H} NMR ($CDCl_3$): δ 20.74 (*C*H_3CO$_2$H), 43.20 (NHCH_2), 70.49 (2 C, CH fc), 73.41 (2 C, CH fc), 73.59 (apparent t, J' = 27 Hz, *C*-P fc), 73.76 (apparent t, J' = 4 Hz, 2 C, CH fc), 127.91 (apparent t, J' = 5 Hz, 4 C, CH PPh_2), 130.57 (2 C, CH PPh_2), 130.91 (apparent t, J' = 25 Hz, 2 C, C_{ipso} PPh_2), 134.17 (apparent t, J' = 6 Hz, 4 C, CH PPh_2), 170.85, 173.09 (2× C=O); 176.19 (CH$_3$*C*O$_2$H); two ferrocene resonances (*C*-CONH and one CH) are obscured by the signal of the solvent. ^{31}P{^{1}H} NMR ($CDCl_3$): δ 16.5 (s). IR (Nujol): ν/cm^{-1} ν_{NH} 3401 m, ν_{NH} 3337 w, amide I 1713 vs, amide I 1625 s, amide II 1547 s, 1437 s, 1304 s, 1255 s, 1167 m, 1101 m, 1059 w, 1028 w, 860 w, 836 w, 750 m, 693 m, 542 m, 512 s, 468 m, 454 w. MS (ESI+): *m*/*z* 1141 ([M + Na]$^+$). Anal. Calcd for $C_{50}H_{46}N_4O_4P_2Fe_2PdCl_2 \cdot 4CH_3CO_2H$: C 51.29, H 4.60, N 4.13. Found: C 51.28, H 4.47, N 4.03.

Preparation of Complex 10. A solution of **1** (97 mg, 0.20 mmol) in chloroform (3 mL) was added to solid [{Pd(μ-Cl)(L^{NC})}$_2$] (55 mg, 0.10 mmol). The resulting mixture was stirred at room temperature for 1 h and filtered (PTFE, 0.45 μm), and the filtrate was layered with pentane (8 mL). Crystallization at room temperature over several days afforded **10** as a dark orange crystalline solid, which was filtered off and dried under vacuum. Yield: 145 mg (90%) of **10**$\cdot 0.35CHCl_3$ (the product retains the reaction solvents).

^{1}H NMR (CD_2Cl_2): δ 2.83 (d, $^4J_{PH}$ = 2.8 Hz, 6 H, NMe_2), 3.70 (s, 3 H, OMe), 4.03 (d, $^3J_{HH}$ = 6.0 Hz, 2 H, NHCH_2), 4.14 (d,$^4J_{PH}$ = 2.4 Hz, 2 H, CH_2NMe$_2$), 4.47 (vq, 2 H, fc), 4.53 (d of vt, 2 H, fc), 4.69 (vt, 2 H, fc), 4.98 (vt, 2 H, fc), 6.27 (ddd, J_{HH} = 1.1, 6.4, 7.7 Hz, 1 H, C_6H_4), 6.36 (tdd, J_{HH} = ca. 7.6, 1.6, 0.6 Hz, 1 H, C_6H_4), 6.81 (td, J_{HH} = 7.2, 1.1 Hz, 1 H, C_6H_4), 7.00 (t, $^3J_{HH} \approx$ 6 Hz, 1 H, NH), 7.02 (dd, J_{HH} = 1.6, 7.3 Hz, 1 H, C_6H_4), 7.31−7.62 (m, 10 H, PPh_2). ^{13}C{^{1}H} NMR (CD_2Cl_2): δ 41.46 (NHCH_2), 50.25 (d, $^3J_{PC}$ = 3 Hz, 2 C, NMe_2), 52.41 (d, $J \approx$ 2 Hz, OMe), 70.59 (2 C, CH fc), 73.79 (2 C, CH fc), 73.96 (d, $^3J_{PC}$ = 3 Hz, *C*H$_2$NMe$_2$), 74.13 (d, J_{PC} = 7 Hz, 2 C, CH fc), 75.76 (d,$^1J_{PC}$ = 59 Hz, *C*-P fc), 77.33 (d, J_{PC} = 10 Hz, 2 C, CH fc), 77.73 (*C*-CONH fc), 122.83 (CH C_6H_4), 124.08 (CH C_6H_4), 125.20 (d, $^4J_{PC}$ = 6 Hz, CH C_6H_4), 128.32 (d, $^3J_{PC}$ = 11 Hz, 4 C, CH PPh_2), 130.99 (d, $^4J_{PC}$ = 2 Hz, 2 C, CH_p PPh_2), 132.22 (d, $^1J_{PC}$ = 49 Hz, 2 C, C_{ipso} PPh_2), 134.77 (d, $^2J_{PC}$ = 12 Hz, 4 C, CH PPh_2), 138.80 (d, J_{PC} = 10 Hz, CH C_6H_4), 147.76 (d, J_{PC} = 2 Hz, C C_6H_4), 152.88 (C C_6H_4), 170.08, 170.90 (2× C=O). ^{31}P{^{1}H} NMR (CD_2Cl_2): δ 32.7 (s). IR (Nujol): ν/cm^{-1} ν_{NH} 3216 s, ν_{CO}(ester) 1742 vs, 1660 w, amide I 1626 vs, 1577 w, amide II 1543 s, 1316 m, 1306 m, 1263 m, 1220 vs, 1195 m, 1169 s, 1097 m, 1040 m, 999 m, 975 m, 866 w, 844 m, 821 m, 762 m, 745 vs, 695 s, 630 m, 545 m, 521 s, 500 m, 475 m, 460 m. MS (ESI+): *m*/*z* 725 ([M − Cl]$^+$). Anal. Calcd for $C_{35}H_{36}N_2O_3PFePdCl \cdot 0.35CHCl_3$: C 52.86, H 4.56, N 3.49. Found: C 52.73, H 4.40, N 3.25.

Preparation of Complex 11. To a solution of **10** (76 mg, 0.10 mmol) in acetonitrile (4 mL) was added a solution of silver(I) perchlorate in the same solvent (21 mg, 0.10 mmol in 2 mL). An off-white precipitate (AgCl) formed immediately. The mixture was stirred for 30 min in the dark and filtered. The filtrate was concentrated to ca. 2 mL under vacuum and layered with diethyl ether. Crystallization at +4 °C for several days afforded **11** as orange crystals, which were filtered off, washed with diethyl ether, and dried under vacuum. Yield: 75 mg (91%).

^{1}H NMR (CD_2Cl_2): δ 2.70 (d, $^4J_{PH}$ = 2.7 Hz, 6 H, NMe_2), 3.63 (s, 3 H, OMe), 4.02 (d,$^3J_{HH}$ = 5.9 Hz, 2 H, NHCH_2), 4.10 (vq, 2 H, fc), 4.14 (d,$^4J_{PH}$ = 2.3 Hz, 2 H, CH_2NMe$_2$), 4.65 (d of vt, 2 H, fc), 4.67 (vt, 2 H, fc), 5.61 (bt vt, 2 H, fc), 6.30 (ddd, J_{HH} = 1.2, 6.6, *ca*. 7.9 Hz, 1 H, C_6H_4), 6.38 (tdd, J_{HH} = ca. 7.9, 1.6, 0.6 Hz, 1 H, C_6H_4), 6.85 (td, J_{HH} = 1.2, 7.3 Hz, 1 H, C_6H_4), 7.01 (dd, J_{HH} = 1.7, 7.4 Hz, 1 H, C_6H_4), 7.37−7.82 (m, 10 H, PPh_2), 8.14 (br t, $^3J_{HH} \approx$ 5.5 Hz, 1 H, NH). ^{13}C{^{1}H} NMR (CD_2Cl_2): δ 42.64 (NHCH_2), 49.75 (d, $^3J_{PC}$ = 2 Hz, 2 C, NMe_2), 52.61 (d, $J \approx$ 2 Hz, OMe), 71.99 (d, $^3J_{PC}$ = 4 Hz, *C*H$_2$NMe$_2$), 72.60 (d, $^1J_{PC}$ = 58 Hz, *C*-P fc), 73.40 (br, 2 C, CH fc), 73.75 (*C*-CONH fc), 74.04 (2 C, CH fc), 74.31 (d, J_{PC} = 7 Hz, 2 C, CH fc), 76.84 (d, J_{PC} = 10 Hz, 2 C, CH fc), 123.47 (CH C_6H_4), 125.20 (CH C_6H_4), 125.94 (d, J_{PC} = 6 Hz, CH C_6H_4), 129.08 (d, J_{PC} = 11 Hz, 4 C, CH PPh_2), 130.13 (d, $^1J_{PC}$ = 49 Hz, 2 C, C_{ipso} PPh_2), 131.88 (d, $^4J_{PC}$ = 2 Hz, 2 C, CH_p PPh_2), 134.81 (d, J_{PC} = 13 Hz, 4 C, CH PPh_2), 139.09 (d, J_{PC} = 13 Hz, CH C_6H_4), 143.06 (d, J_{PC} = 4 Hz, C C_6H_4), 148.37 (d, J_{PC} = 2 Hz, C C_6H_4), 169.48 (*C*O$_2$Me), 175.27 (CONH). ^{31}P{^{1}H} NMR (CD_2Cl_2): δ 30.9 (s). IR (Nujol): ν/cm^{-1} ν_{NH} 3358 m, ν_{CO}(ester) 1754 vs, amide I 1598 vs, amide II 1578 s, 1321 m, 1216 vs, 1180 s, 1167 m, 1126 vs, 1098 vs, 1067 vs, 1046 s, 1031 s, 1010 m, 996 m, 978 m, 931 m, 844 m, 814 m, 766 m, 750 vs, 699 s, 691 m, 622 s, 538 m, 520 s, 501 s, 494 m, 484 s, 468 m. MS (ESI+): *m*/*z* 725 ([M − ClO_4]$^+$; i.e., the cation). Anal. Calcd for $C_{35}H_{36}N_2O_7PFePdCl$: C 50.93, H 4.40, N 3.40. Found: C 50.84, H 4.49, N 3.60.

Preparation of Complex 12. Compound **10** (76 mg, 0.10 mmol) and potassium *tert*-butoxide (22 mg, 0.20 mmol) were dissolved in dichloromethane (5 mL), and the mixture was stirred at room temperature overnight. Then, hexane (5 mL) and diatomaceous earth (Celite; ca. 100 mg) were added, and stirring was continued for 10 min. The mixture was filtered (PTFE, 0.45 μm), and the filtrate was evaporated under vacuum. The solid residue was dissolved in ethyl acetate (2 mL) and layered with hexane. Crystallization at room temperature over several days afforded **12** as dark orange crystals. The separated product was filtered off, washed with hexane, and dried under vacuum. Yield: 43 mg (59%).

^{1}H NMR (CD_2Cl_2): δ 2.59 (d, $^4J_{PH}$ = 2.1 Hz, 3 H, NMe_2), 2.68 (d, $^4J_{PH}$ = 3.2 Hz, 3 H, NMe_2), 3.32 (s, OMe), 3.44 (dd, $^4J_{PH}$ = 3.8, $^2J_{HH}$ = 13.1 Hz, 1 H, CH_2NMe$_2$), 3.48 (dq, J = 2.7, 1.3 Hz, 1 H, fc), 3.82 (d, $^2J_{HH}$ = 15.7 Hz, 1 H, CONCH_2), 4.09 (m, 1 H, fc), 4.16 (dt, J = 1.2. 2.6 Hz, 1 H, fc), 4.30 (d, $^2J_{HH}$ = 15.7 Hz, 1 H, CONCH_2), 4.50 (dt, J = 1.5, 2.5 Hz, 1 H, fc), 4.68 (m, 2 H, fc), 4.85 (d, $^2J_{HH}$ = 13.1 Hz, 1 H, CH_2NMe$_2$), 4.91 (dt, J = 2.7, 1.5 Hz, 1 H, fc), 6.29 (t of m, J = 7.5 Hz, 1 H, C_6H_4), 6.34 (ddd, J = 1.4, 5.5, 7.6 Hz, 1 H, C_6H_4), 6.44 (dt, J = 2.6, 1.3 Hz, 1 H, fc), 6.74 (td, J = 7.3, 1.3 Hz, 1 H, C_6H_4), 6.99 (d of unresolved t, J = 7.3 Hz, 1 H, C_6H_4), 6.99−8.09 (partly broad complex m, 10 H, PPh_2). ^{13}C{^{1}H} NMR (CD_2Cl_2): δ 49.49 (d, $^3J_{PC}$ = 2 Hz, NMe_2), 50.12 (d, $^3J_{PC}$ = 2 Hz, NMe_2), 51.11 (d, $J \approx$ 1 Hz, OMe), 51.23 (CON*C*H$_2$), 69.63 (CH fc), 69.80 (d, J_{PC} = 6 Hz, CH fc), 71.89 (CH fc), 72.77 (d, $^1J_{PC}$ = 63 Hz, *C*-P fc), 72.94 (CH fc), 74.17 (d, $^3J_{PC}$ = 3 Hz, *C*H$_2$NMe$_2$), 75.40 (d, J_{PC} = 7 Hz, CH fc), 75.60 (d, J_{PC} = 8 Hz, CH fc), 77.23 (dd, $J \approx$ 6 and 2 Hz, CH fc), 80.36 (d, J_{PC} = 12 Hz, CH fc), 81.89 (*C*-CON fc), 122.67 (CH C_6H_4), 123.71 (CH C_6H_4), 125.05 (d, J_{PC} = 5 Hz, CH C_6H_4), ca. 127.9 (very br m, 2 C, CH PPh_2), 129.09 (d, J_{PC} = 11 Hz, 2 C, CH PPh_2), 130.27 (d, $^4J_{PC}$ = 2 Hz, CH_p PPh_2), 130.55 (d, $^1J_{PC}$ = 45 Hz, C_{ipso} PPh_2), 131.3 (br s, CH PPh_2), 131.83 (d, $^4J_{PC}$ = 2 Hz, CH_p PPh_2), 133.06 (d, $^1J_{PC}$ = 51 Hz, C_{ipso} PPh_2), 135.2 (br s, CH PPh_2), 136.50 (d, J_{PC} = 15 Hz, 2 C, CH PPh_2), 140.37 (d, J_{PC} = 10 Hz, CH C_6H_4), 148.50 (d, J_{PC} = 2 Hz, C C_6H_4), 153.59 (d, J_{PC} = 4 Hz, C C_6H_4), 173.02

(CO_2Me), 174.53 (br, NC═O). $^{31}P\{^1H\}$ NMR (CD_2Cl_2): δ 33.6 (s). IR (Nujol): ν/cm^{-1} 3058 w, 2360 w, ν_{CO} (ester) 1724 vs, 1653 w, amide I 1565 vs, 1554 s, 1318 m, 1243 m, 1203 w, 1193 w, 1160 m, 1100 m, 1028 m, 906 w, 843 m, 838 m, 813 m, 740 s, 697 s, 531 m, 518 s, 509 s, 481 m. MS (ESI+): *m*/*z* 725 ([M + H]$^+$). HR-MS (FAB+): calcd for $C_{35}H_{36}N_2O_3P^{56}FePd$ ([M + H]$^+$) 725.0848, found 725.0858. Anal. Calcd for $C_{35}H_{35}N_2O_3PFePd$: C 57.99, H 4.87, N 3.87. Found: C 57.70, H 4.94, N 3.57.

Reaction of 12 with HCl. Complex **12** (11 mg, 15 μmol) was dissolved in dichloromethane (2 mL), and to the resulting solution was added a methanolic solution of HCl (21 μL 0.7 M, 15 μmol). The mixture was stirred at room temperature for 2 h and evaporated. A subsequent analysis by ^1H and $^{31}P\{^1H\}$ NMR spectroscopy indicated a complete regeneration of **10**.

Suzuki−Miyaura Cross-Coupling. A General Procedure. A reaction vessel was charged with palladium(II) acetate (1 mg, 5 μmol), the phosphine ligand (6 μmol; if appropriate), potassium carbonate (276 mg, 2 mmol), phenylboronic acid (146 mg, 1.2 mmol), and 4-bromotoluene (171 mg, 1.0 mmol), flushed with argon, and sealed with a rubber septum. Then, solvent was introduced (5 mL), and the mixture was transferred to an oil bath preheated to 80 °C and stirred at this temperature for the given reaction time. Conversion was monitored by withdrawing small aliquots and recording ^1H NMR spectra. The samples from organic solvents were filtered through a 0.45 μm PTFE syringe filter and diluted with $CDCl_3$. Samples from experiments in aqueous media were extracted into diethyl ether, and the extract was dried ($MgSO_4$), filtered, and diluted with $CDCl_3$. In cases of complete conversion, the reaction mixture was extracted with diethyl ether, and the extract was dried ($MgSO_4$) and passed through a short silica column, eluting with hexane/ethyl acetate (1:1 v/v). Subsequent evaporation afforded analytically pure **13** as a white solid. The compound was characterized by a comparison with an authentic sample.

X-ray Crystallography. Crystals suitable for single-crystal X-ray diffraction analysis were grown from ethyl acetate/hexane (**2**: orange block, 0.35 × 0.58 × 0.60 mm^3; **3**: orange prism, 0.08 × 0.24 × 0.36 mm^3; **6**: orange bar, 0.15 × 0.18 × 0.55 mm^3; **12**: orange block, 0.22 × 0.27 × 0.48 mm^3), toluene/hexane (**4**: orange prism, 0.37 × 0.45 × 0.62 mm^3), acetone/diethyl ether (**10**: orange bar, 0.08 × 0.10 × 0.40 mm^3), and from acetonitrile/diethyl ether (**11**: orange block, 0.13 × 0.30 × 0.33 mm^3). Crystals of **9** were grown from acetic acid/diethyl ether; **9a** resulted by recrystallization of **9** from chloroform/diethyl ether (**9**: orange plate, 0.03 × 0.15 × 0.20 mm^3; **9a**: orange plate, 0.03 × 0.25 × 0.55 mm^3).

Full-set diffraction data ($\pm h$, $\pm k$, $\pm l$) of **3** were collected on an Oxford Diffraction XCalibur 2 diffractometer with Sapphire 2 CCD detector equipped with an Oxford Instruments Cryojet HT Cooler (Oxford Cryosystems). The data for all other compounds were collected with a Nonius KappaCCD diffractometer equipped with a Cryostream Cooler (Oxford Cryosystems). All measurements were performed at 150(2) K using graphite-monochromatized Mo Kα radiation (λ = 0.71073 Å). When appropriate, the intensity data were corrected for absorption by using the absorption correction routines incorporated in the diffractometer software; the ranges of transmission factors (TF) are given in Table 9.

The structures were solved by direct methods (SIR97[46]) and refined by full-matrix least-squares on F^2 (SHELXL97[47]). Non-hydrogen atoms were refined with anisotropic thermal motion parameters. Amide hydrogens were identified on the difference electron density maps and refined freely (**2**, **3**, **11**) or as a riding atoms (**4**, **6**, **10**, **9**, **9a**). Other hydrogen atoms were included in the calculated positions and refined as riding atoms with U_{iso}(H) assigned to a multiple of U_{eq} of their bonding atom.

Particular comments on structure refinement are as follows: The large residual electron density can be explained by statistical disorder of the phosphinylated cyclopentadienyl ring, $C_5H_4PPh_2$. The largest positive difference electron density peak attributable to the P atom in the less populated orientation lies in the plane of the cyclopentadienyl ring and has a similar distance from Fe as the major component. Refinement over two positions proved impossible due to low abundance of the less populated orientation and overlaps. Complex **10** crystallizes with the symmetry of the chiral space group $Pca2_1$ but as a racemic twin. The contributions of the enantiomeric cells refined to 0.27:0.73. Finally, the perchlorate anion in the structure of **11** is partly disordered and was modeled with its Cl, O(4), and O(5) atoms as invariant pivots and with two positions for each O(6) and O(7).

Relevant crystallographic data are given in Table 9. Geometric parameters and structural drawings were obtained with a recent version of the Platon program.[48] All calculated values are rounded with respect to their estimated standard deviations (esd's) given with one decimal; parameters involving atoms in constrained positions (typically hydrogens) are given without esd's. CCDC 723117−723125 contain the supplementary crystallographic data for this paper. These data can be obtained free of charge from The Cambridge Crystallographic Data Centre via www.ccdc.cam.ac.uk/data_request/cif.

Acknowledgment. This work is a part of the long-term research project supported by the Ministry of Education, Youth and Sports of the Czech Republic (project nos. MSM0021620857 and LC06070).

Supporting Information Available: Alternative views of the molecular structures of **9** and **9a** and overlaps of the crystallographically independent molecules for complexes **10** and **12**. This material is available free of charge via the Internet at http://pubs.acs.org.

OM900209J

(46) Altomare, A.; Burla, M. C.; Camalli, M.; Cascarano, G. L.; Giacovazzo, C.; Guagliardi, A.; Moliterni, A. G. G.; Polidori, G.; Spagna, R. *J. Appl. Crystallogr.* **1999**, *32*, 115.

(47) Sheldrick, G. M. *SHELXL97. Program for Crystal Structure Refinement from Diffraction Data*; University of Goettingen: Germany, 1997.

(48) (a) Spek, A. L. *Platon—A Multipurpose Crystallographic Tool*; Utrecht University: Utrecht, The Netherlands, 2007. For a reference, see: (b) Spek, A. L. *J. Appl. Crystallogr.* **2003**, *36*, 7.